

THESIS

SIDELOBE REDUCTION IN PEANO-GOSPER FRACTAL ARRAYS USING GENETIC ALGORITHMS

META POLPASEE

**GRADUATE SCHOOL, KASETSART UNIVERSITY
2007**



THESIS APPROVAL
GRADUATE SCHOOL, KASETSART UNIVERSITY

Master of Engineering (Electrical Engineering)
DEGREE

Electrical Engineering
FIELD

Electrical Engineering
DEPARTMENT

TITLE: Sidelobe Reduction in Peano-Gosper Fractal Arrays using Genetic Algorithms

NAME: Mr. Meta Polpasee

THIS THESIS HAS BEEN ACCEPTED BY

Handwritten signature of Nuttaka Homsup.

THESIS ADVISOR

(Associate Professor Nuttaka Homsup, Ph.D.)

Handwritten signature of Waroth Kuhirun.

COMMITTEE MEMBER

(Assistant Professor Waroth Kuhirun, Ph.D.)

Handwritten signature of Wiroj Homsup.

COMMITTEE MEMBER

(Associate Professor Wiroj Homsup, Ph.D.)

Handwritten signature of Mongkol Raksapatcharawon.

DEPARTMENT HEAD

(Associate Professor Mongkol Raksapatcharawon, Ph.D.)

APPROVED BY THE GRADUATE SCHOOL ON 21 / 03 / 07

Handwritten signature of Vinai Artkongharn.

DEAN

(Associate Professor Vinai Artkongharn, M.A.)

THESIS

SIDELobe REDUCTION IN PEANO-GOSPER FRACTAL ARRAYS
USING GENETIC ALGORITHMS

META POLPASEE

A Thesis Submitted in Partial Fulfillment of
the Requirements for the Degree of
Master of Engineering (Electrical Engineering)
Graduate School, Kasetsart University

2007

Meta Polapsee 2007: Sidelobe Reduction in Peano-Gosper Fractal Arrays using Genetic Algorithms. Master of Engineering (Electrical Engineering), Major Field: Electrical Engineering, Department of Electrical Engineering. Thesis Advisor: Associate Professor Nuttaka Homsup, Ph.D. 65 pages.

In recent years, engineers have exploited nature-based concepts in antenna designs. The Fractal Array is a class of antenna arrays which are designed using fractal geometry (The geometric characterization of the simplest fractals is self-similarity: the shape is made of smaller copies of itself. The copies are similar to the whole: same shape but different size). The first application of fractals in the field of antenna engineering was reported by Kim and Jaggard. Broadband antenna arrays with low sidelobe levels can be possibly generated using fractal geometry. Although the strategic arrangement of antenna array elements can generate low sidelobe level, reducing sidelobe levels is a very difficult problem. The antenna arrays with low sidelobe levels can be synthesized using many analytical methods including the Chebyshev method and Taylor method. In the synthesis of multi-element antenna arrays, genetic algorithm, a global optimization and widely used technique can search through a large solution space.



Student's signature



Thesis Advisor's signature

14 / 9 / 07

ACCKNOWLEDGEMENT

The author would like to thank Associate Professor Nuttaka Homsup for his advice and assistance, in adjusting and correcting the contents and for serving as his major advisor. The author is deeply grateful for Assistant Professor Waroth Kuhirun who gave useful suggestions for this research. The author wishes to express his appreciation to Mr. Terapass Jiranorawiss for his kindly support in giving useful suggestions. Finally, I would like to dedicate all my works to my family who encourages me and gives me a chance to experience in the world of living and learning

Meta Polpasee

February 2007

TABLE OF CONTENTS

	Page
TABLE OF CONTENTS	i
LIST OF TABLES	ii
LIST OF FIGURES	iii
INTRODUCTION	1
LITERATURE REVIEWS	17
MATERIAL AND METHOD	20
Materials	20
Method	20
RESULT AND DISCUSSIONS	26
CONCLUSION AND RECOMMENDATION	59
LITERATURE CITED	60
CURRICULUM VITAE	64

LIST OF TABLES

Table		Page
1	Comparison of the sidelobe levels in dB of the genetically optimized stage 3 Peano-Gosper fractal arrays with different parameters for both approaches.	58

LIST OF FIGURES

Figure		Page
1	Cantor Set	4
2	Koch Curve	5
3	Sierpinski gasket	5
4	Sierpinski carpet	6
5	Example of Binary Encoding	11
6	Example of Permutation Encoding	11
7	Example of Value Encoding	12
8	Graph of fitness	13
9	Example of Rank Selection (Before and After)	14
10	Example of Crossover	14
11	Example of Mutation	15
12	The Geometry for planar arrays of isotropic sources	17
13	Linear plot of power pattern and its associated lobes	18
14	The Peano-Gosper curve initiator	20
15	The Peano-Gosper curve generator	21
16	The first three stages in the construction of self-avoiding Peano-Gosper curve. The initiator is show as the dashed line superimposed on the stage 1generator. The generator (unscaled) is shown again in (b) as the dashed curve superimposed on the stage 2Peano-gosper curve	22
17	Flow Chart of Methodologies case 1	24
18	Flow Chart of Methodologies case 1	25
19	The Peano-Gosper fractal arrays configurations and their relative current excitation for the stages of growth 1, 2 and 3, respectively	26

LIST OF FIGURES (cont'd)

Figure		Page
20	Element location for the (a) stage 1, (b) stage 2, and (c) stage 3 Peano-Gosper fractal arrays. A uniform spacing of d_{\min} is assumed between consecutive arrays elements which is the same for each stage, minimum spacing is $\lambda/2$, maximum current excitation is one	27
21	Evolution diagram of Genetically Optimized a Stage3: Peano-Gosper Fractal Array minimum spacing is $\lambda/2$, maximum current excitation is one	28
22	Plot of the normalized stage 3 Peano-Gosper fractal array, genetically optimized array factor versus (a) ϕ for $\theta = 90^\circ$ and (b) θ for $\phi = 90^\circ$ where minimum distance equal $\lambda/2$ and maximum current excitation equal one	28
23	The normalized radiation pattern in dB for stage 3 of Peano-Gosper fractal array from Figure 20c with a minimum spacing is $\lambda/2$, maximum current excitation is one and main beam steered to $\theta = 0$ degrees and $\phi = 90^\circ$ degrees. (a) Radiation Pattern, and (b) Top View	29
24	Element location for the (a) stage 1, (b) stage 2, and (c) stage 3 Peano-Gosper fractal arrays. A uniform spacing of d_{\min} is assumed between consecutive arrays elements which is the same for each stage, minimum spacing is $\lambda/2$, maximum current excitation is ten.	31
25	Evolution diagram of Genetically Optimized a Stage3: Peano-Gosper Fractal Array, minimum spacing is $\lambda/2$, maximum current excitation is ten.	32
26	Plot of the normalized stage 3 Peano-Gosper fractal array, genetically optimized array factor versus (a) ϕ for $\theta = 90^\circ$ and (b) θ for $\phi = 90^\circ$ where minimum distance equal $\lambda/2$ and maximum current excitation equal ten.	32
27	Top view of the normalized radiation pattern in dB for stage of Peano-Gosper fractal array of isotropic elements from Figure 24c with a minimum spacing is $\lambda/2$, maximum current excitation is ten and main beam steered to $\theta = 0$ degrees and for $\phi = 90^\circ$ degrees.	33

LIST OF FIGURES (cont'd)

Figure		Page
28	Element location for the (a) stage 1, (b) stage 2, and (c) stage 3 Peano-Gosper fractal arrays. A uniform spacing of d_{\min} is assumed between consecutive arrays elements which is the same for each stage, minimum spacing is λ , maximum current excitation is one.	35
29	Evolution diagram of Genetically Optimized a Stage3: Peano-Gosper Fractal Array, minimum spacing is λ , maximum current excitation is one.	36
30	Plot of the normalized stage 3 Peano-Gosper fractal array, genetically optimized array factor versus (a) ϕ for $\theta = 90^\circ$ and (b) θ for $\phi = 90^\circ$ where minimum distance equal λ and maximum current excitation equal one	36
31	The normalized radiation pattern in dB for stage 3 of Peano-Gosper fractal array from Figure 28c with a minimum spacing is λ , maximum current excitation is one and main beam steered to $\theta = 0$ degrees and $\phi = 90^\circ$ degrees. (a) Radiation Pattern, and (b) Top View	37
32	Element location for the (a) stage 1, (b) stage 2, and (c) stage 3 Peano-Gosper fractal arrays. A uniform spacing of d_{\min} is assumed between consecutive arrays elements which is the same for each stage, minimum spacing is λ , maximum current excitation is ten	39
33	Evolution diagram of Genetically Optimized a Stage3: Peano-Gosper Fractal Array, minimum spacing is λ , maximum current excitation is ten.	40
34	Plot of the normalized stage 3 Peano-Gosper fractal array, genetically optimized array factor versus (a) ϕ for $\theta = 90^\circ$ and (b) θ for $\phi = 90^\circ$ where minimum distance equal λ and maximum current excitation equal ten.	40
35	The normalized radiation pattern in dB for stage 3 of Peano-Gosper fractal array from Figure 32c with a minimum spacing is λ , maximum current excitation is ten and main beam steered to $\theta = 0$ degrees and $\phi = 90^\circ$ degrees. (a) Radiation Pattern, and (b) Top View.	41

LIST OF FIGURES (cont'd)

Figure	Page	
36	Element location for the (a) stage 1, (b) stage 2, and (c) stage 3 Peano-Gosper fractal arrays. A uniform spacing of d_{\min} is assumed between consecutive arrays elements which is the same for each stage, minimum spacing is $\lambda/2$, maximum current excitation is one	43
37	Evolution diagram of Genetically Optimized a Stage3: Peano-Gosper Fractal Array, minimum spacing is $\lambda/2$, maximum current excitation is one.	44
38	Plot of the normalized stage 3 Peano-Gosper fractal array, genetically optimized array factor versus (a) ϕ for $\theta = 90^\circ$ and (b) θ for $\phi = 90^\circ$ where minimum distance equal $\lambda/2$ and maximum current excitation equal one.	44
39	The normalized radiation pattern in dB for stage 3 of Peano-Gosper fractal array from Figure 36c with a minimum spacing is $\lambda/2$, maximum current excitation is one and main beam steered to $\theta = 0$ degrees and $\phi = 90^\circ$ degrees. (a) Radiation Pattern, and (b) Top View.	45
40	Element location for the (a) stage 1, (b) stage 2, and (c) stage 3 Peano-Gosper fractal arrays. A uniform spacing of d_{\min} is assumed between consecutive arrays elements which is the same for each stage, minimum spacing is $\lambda/2$, maximum current excitation is ten.	47
41	Evolution diagram of Genetically Optimized a Stage3: Peano-Gosper Fractal Array, minimum spacing is $\lambda/2$, maximum current excitation is ten	48
42	Plot of the normalized stage 3 Peano-Gosper fractal array, genetically optimized array factor versus (a) ϕ for $\theta = 90^\circ$ and (b) θ for $\phi = 90^\circ$ where minimum distance equal $\lambda/2$ and maximum current excitation equal ten.	48
43	The normalized radiation pattern in dB for stage 3 of Peano-Gosper fractal array from Figure 40c with a minimum spacing is $\lambda/2$, maximum current excitation is ten and main beam steered to $\theta = 0$ degrees and $\phi = 90^\circ$ degrees. (a) Radiation Pattern, and (b) Top View.	49

LIST OF FIGURES (cont'd)

Figure		Page
44	Element location for the (a) stage 1, (b) stage 2, and (c) stage 3 Peano-Gosper fractal arrays. A uniform spacing of d_{\min} is assumed between consecutive arrays elements which is the same for each stage, minimum spacing is λ , maximum current excitation is one.	51
45	Evolution diagram of Genetically Optimized a Stage3: Peano-Gosper Fractal Array, minimum spacing is λ , maximum current excitation is one.	52
46	Plot of the normalized stage 3 Peano-Gosper fractal array, genetically optimized array factor versus (a) ϕ for $\theta = 90^\circ$ and (b) θ for $\phi = 90^\circ$ where minimum distance equal λ and maximum current excitation equal one.	52
47	The normalized radiation pattern in dB for stage 3 of Peano-Gosper fractal array from Figure 44c with a minimum spacing is λ , maximum current excitation is one and main beam steered to $\theta = 0$ degrees and $\phi = 90^\circ$ degrees. (a) Radiation Pattern, and (b) Top View.	53
48	Element location for the (a) stage 1, (b) stage 2, and (c) stage 3 Peano-Gosper fractal arrays. A uniform spacing of d_{\min} is assumed between consecutive arrays elements which is the same for each stage, minimum spacing is λ , maximum current excitation is ten.	55
49	Evolution diagram of Genetically Optimized a Stage3: Peano-Gosper Fractal Array, minimum spacing is λ , maximum current excitation is ten.	56
50	Plot of the normalized stage 3 Peano-Gosper fractal array, genetically optimized array factor versus (a) ϕ for $\theta = 90^\circ$ and (b) θ for $\phi = 90^\circ$ where minimum distance equal λ and maximum current excitation equal ten.	56
51	The normalized radiation pattern in dB for stage 3 of Peano-Gosper fractal array from Figure 48c with a minimum spacing is λ , maximum current excitation is ten and main beam steered to $\theta = 0$ degrees and $\phi = 90^\circ$ degrees. (a) Radiation Pattern, and (b) Top View.	57

SIDELOBE REDUCTION IN PEANO-GOSPER FRACTAL ARRAYS USING GENETIC ALGORITHMS

INTRODUCTION

In recent years, engineers have exploited nature-based concepts in antenna designs. The Fractal Array is a class of antenna arrays which are designed using fractal geometry. What is fractal geometry? The first application of fractals in the field of antenna engineering was reported by Kim and Jaggard. Broadband antenna arrays with low sidelobe levels can be possibly generated using fractal geometry. Although the strategic arrangement of antenna array elements can generate low sidelobe level, reducing sidelobe levels is a very difficult problem. The antenna arrays with low sidelobe levels can be synthesized using many analytical methods including the Chebyshev method and Taylor method. In the synthesis of multi-element antenna arrays, genetic algorithm, a global optimization and widely used technique can search thorough a large solution space.

Genetic Algorithms is an optimization method based upon the theory of natural selection. The theory concern with natural selection chromosome crossover, and gene mutation over a large population of antennas in order to find the most suitable solutions. The process can be used for creating and collecting the minimum or maximum solution. Genetic Algorithm is useful for optimizing. The algorithm is well suited for a large optimization problem because there is no limitation for the number of optimized variables.

The objectives of this research are listed as following:

The objective of this research is to investigate a type of nature - based antenna array design. The design is to strategically position antenna elements on the Peano - Gosper Fractal Array using Genetic Algorithms for optimizing overall sidelobe level. This thesis shows some examples of fractal arrays optimized by reducing sidelobe level.

The scopes of study of this research are conducted based on the following:

1. To create a source code for solving optimization problems on MATLAB.
2. To develop a GA code for optimizing (minimizing) sidelobe level of fractal Antenna Arrays.
3. To optimize sidelobe level of various Fractal Antenna Arrays using Genetic Algorithm.

LITERATURE REVIEW

In most modern communication systems, high performance antennas, one of the critical parts, are required. The main objective in designing antennas is to optimize (improve) the performance of antennas. There are numerous concepts we can exploit for optimizing antenna performance; two of which are fractal geometry and genetic algorithm, a nature-based optimization technique.

1. Background of Fractal

1.1. Fractal Geometries

“Fractal” was coined by B.B Mandelbrot, a French mathematician. He originally introduced “Fractal” in his book, “The Fractal Geometry of Nature”. “Fractal”, derived from a Latin word, “fractus” literally means “broken” or “fracture”. In our context, a Fractal is a geometrical object which holds a property called, “Self-Similarity”. This means that parts of the whole structure are similar to the whole.

Fractal geometry was originated to describe complex shapes in nature that cannot be easily characterized using classical Euclidean geometry. Mathematicians who played a major role in developing fractal geometry are, for example, Cantor (1872), Peano (1890), Hilbert (1891), Koch (1904), Sierpinski (1916), Julia (1918). However, applications in engineering of fractal geometry had not been found until the pioneering work of Mandelbrot (1970). Since 1980s, fractal have been investigated in physics and engineering. Kim and Jaggard reported the first application of fractal geometry in designing antennas. Fractal Geometry and electromagnetic theory were amalgamated for a new methodology to design of low sidelobe level arrays based on the theory of random fractals.

Fractals which are generated by an iterative algorithm comprising of dilations and translations of an initial set are said to be deterministic. Several examples of deterministic fractals will be described in next section.

1.2. Examples of fractal geometry

The Cantor set

The Cantor set is shown in Figure 1. It can be generated by an iterative procedure. At stage 0, begin with an interval $[0, 1]$ called C_0 . Remove the open middle third $(1/3, 2/3)$ from C_0 to obtain $C_1 = [0, 1/3] \cup [2/3, 1]$. At stage 1, Remove the open middle third from each remaining interval to obtain $C_2 = [0, 1/9] \cup [2/9, 1/3] \cup [2/3, 7/9] \cup [8/9, 1]$. For further stages, iterate the previous step. To obtain C_{n+1} , remove the open middle third of the remaining intervals of C_n . As n approaches ∞ , we obtain a set of points called the Cantor Set.



Figure 1 Cantor Set

Koch curve

Another example of fractals is The Koch Curve, shown in Figure 2. It can be generated by an iterative procedure. At stage 0, begin with a straight line. At stage 1, divide it into three equal segments and replace the middle segment by the two remaining sides of an equilateral triangle of the same length as the segment being removed. For further stages, iterate the previous procedure. As the procedure continues infinite times, the remaining structure is so-called “Koch curve”.

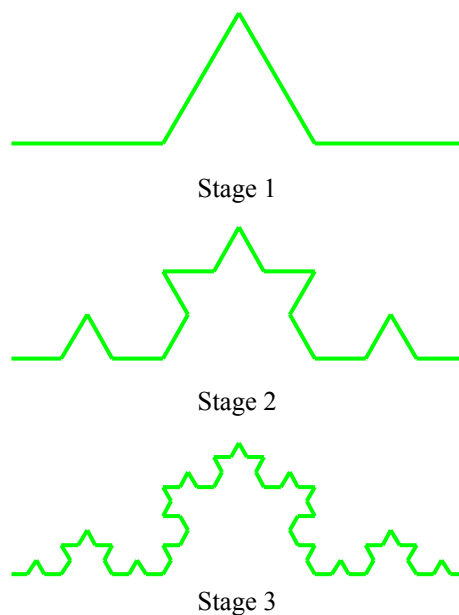


Figure 2 Koch Curve

The Sierpinski gasket

The Sierpinski gasket triangle is an example of deterministic fractals. It holds a property, which is common to all other fractals, called self-similarity; for whatever part of the triangle we take, if we magnify it, we will find exactly the same triangle in it. The Sierpinski gasket for various stages is shown in Figure 3. The procedure for generating the Sierpinski gasket is as follows. At stage 0, begin with an equilateral triangle. Then use the midpoints of each side as the vertices of a new triangle, which we then remove from the equilateral triangle. For further stages, use the midpoints of each side as the vertices of a new triangle, which we then remove from each of the remaining triangles in the previous stage.



Figure 3 Sierpinski gasket

The Sierpinski carpet

The Sierpinski carpet is an example of deterministic fractals. The Sierpinski carpet is essentially the generalized version of the Cantor set into two dimensions. To generate the Sierpinski carpet, begin with a square, subdivide it into nine smaller congruent squares of which we remove the open central square, then subdivide the eight remaining squares into nine smaller congruent squares in each of which we remove the open central square. As the procedure continues infinite times, we obtain the Sierpinski carpet.

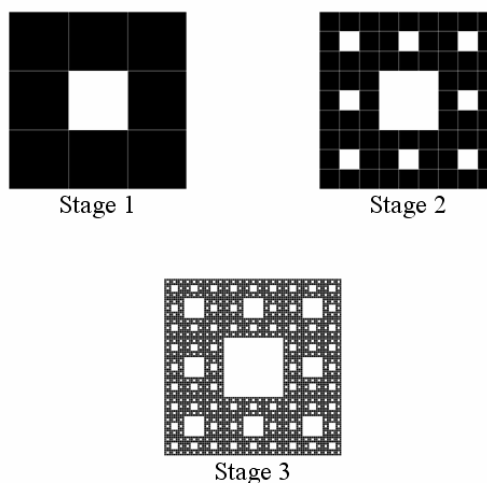


Figure 4 Sierpinski carpet

Some of the properties of fractals are qualitatively linked to the features of antennas associated with the fractals geometries using them. It is envisaged that the above description of these properties would shed light into a better understanding of such connection. In the following sub-section a brief introduction is provide on the use of fractal in science and engineering, and antenna engineering in particular.

1.3. Fractal in Antenna Engineering

The primary motivation of fractal antenna engineering is to extend antenna design and synthesis concepts beyond Euclidean geometry. This thesis concerns antenna array synthesis using fractal geometry to obtain antenna arrays with special features. It is widely known that properties of antenna arrays are dominated by the arrangement of antenna elements and their relative current excitation rather than by the structure of each individual element. Since the array spacing between adjacent elements in terms of wavelength depends on the operating frequency, most of the conventional antenna arrays have limited bandwidth. It has been found that the concept of self-similarity property of fractals can help improve design of such arrays.

2. Genetic Algorithms overview

Evolution computing was introduced in the 1960s by I. Rechenberg in his work "Evolution strategies". His idea was then developed by other researchers. The Genetic Algorithms were invented and developed by Prof. John Holland and his students over the course at the University of Michigan between 1960s and 1970s. Subsequently, it has been made widely popular by one of his students, Prof. David Golde (at the University of Illinois), who was able to solve a difficult problem involving the control of gas-pipeline transmission for his dissertation. The genetic algorithm (GA) is robust, stochastic search method, modeled based on the principles of genetics and mimic the natural process of selection (Darwinian Theory of evolution). The theories of evolution and nature selection were first proposed by Charles Darwin, to explain his observation of plants and animals in the nature of the world. Darwin observed that variations are introduced into a population with each new generation, the less-fit individuals tend to die off in the competition for food, and this survival of the fittest principle leads to improvements in the species.

Some of the advantages of a GA include that it

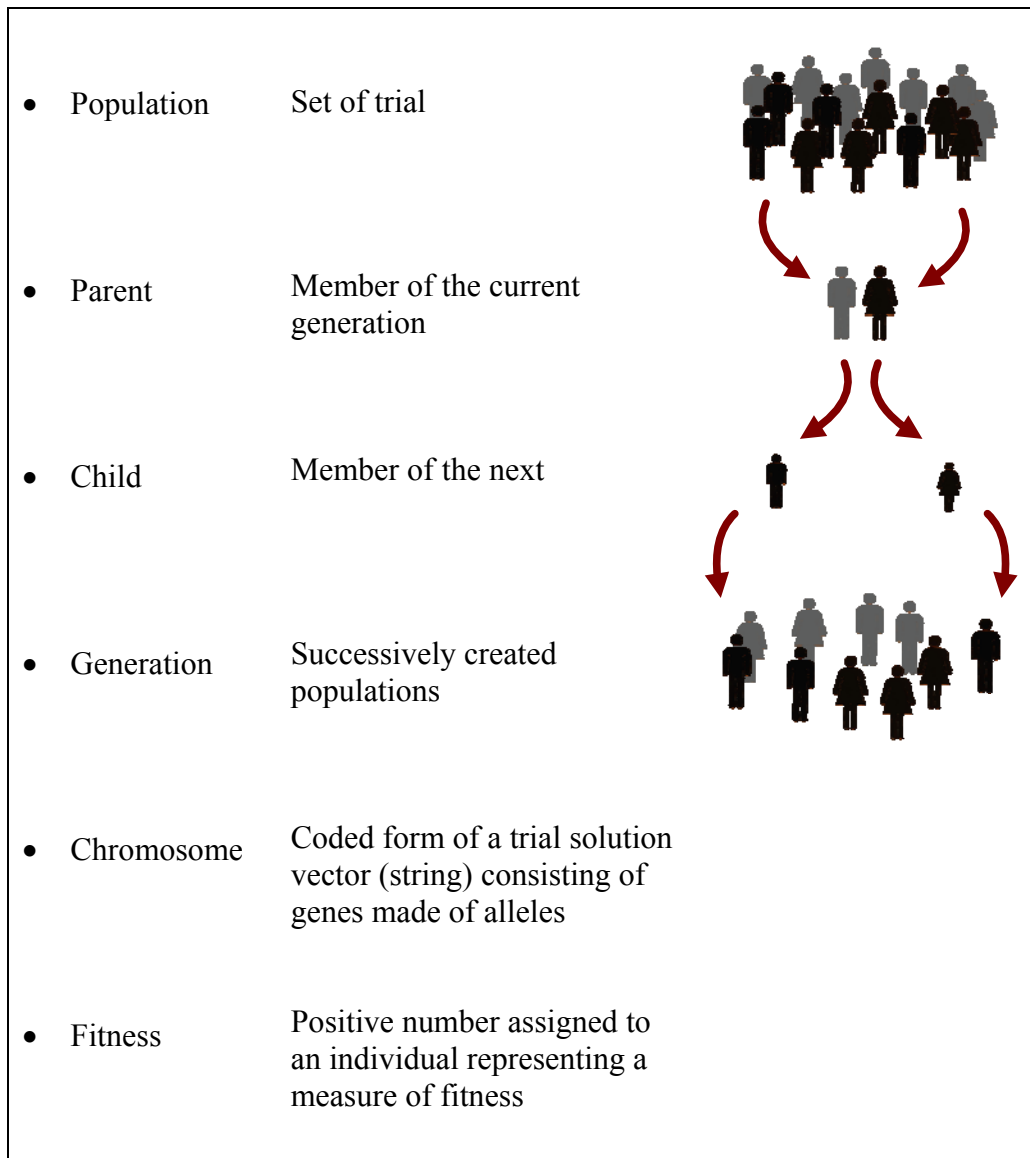
- Optimizes with continuous or discrete variable
- Doesn't require derivative information,
- Simultaneously searches from a wide sampling of the cost surface,
- Deals with a large number of variables,

- Is well suited for parallel computers,
- Optimizes variable with extremely complex cost surface(they can jump out a local minimum),
- Provide a list of optimum variable, not just a single solution,
- May encode the variable so that optimization is done with the encoded variable
- Work with numerically generated data , experimental data, or analytical function

Outline of the Genetic Algorithm

1. Generate a random population of n chromosomes which are suitable solutions.
2. Establish a method to evaluate the fitness $f(x)$ of each chromosome x in the population
3. Create a new population by repeating the following steps until the new population is complete
 - Selection - Select from the population according to some fitness scheme.
 - Crossover - New offspring formed by a crossover with the parents
 - Mutation - With a mutation probability mutate new offspring at each locus (position in chromosome).
4. Create new population from the newly generated population by repeating step 3.

A list of some of the commonly encountered Genetic Algorithms terms relating to the optimization problem is presented below



2.1. Biological Background

Chromosomes

All living organisms consist of cells. In each cell there is the same set of chromosomes. Chromosomes are strings of DNA and serve as a model for the whole organism. A chromosome consists of genes, blocks of DNA. Each gene encodes a particular protein. Basically, each gene encodes a trait, for example eye color. Possible settings for a trait (e.g. blue, brown) are called alleles. Each gene has its own position in the chromosome. This position is called locus. A complete set of genetic material (all chromosomes) is called genome. A particular set of genes in genome is called the genotype.

Reproduction

During reproduction, the first thing that occurs is recombination (or cross-over). Genes from the parents combine in some way to create a whole new chromosome. The newly created offspring can then be mutated. Mutation means that the elements of DNA are a bit changed. These changes are mainly caused by errors in copying genes from parents.

Fitness

The fitness of an organism is measured by the success of the organism in its life.

Evolution

Evolution is a process that results in changes in a population over many generations by cross-over and mutation

2.2. Genetic Operators

The genetic operators and their significance can now be explained. The description will be in terms of a traditional GA without any problem-specific modifications. The operators that will be discussed include Encoding, selection, crossover, mutation, fitness scaling and inversion.

Encoding of a chromosome

A Chromosome should in some way contain information about solution that it represents.

(a) Binary Encoding

One way of encoding is a binary string. The chromosome could look like this:

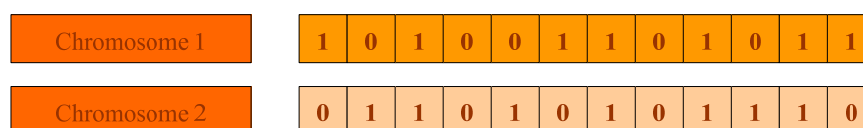


Figure 5 Example of Binary Encoding

Each bit in the string can represent a character of the solution or it could represent whether or not a character is present. Another possibility is that the chromosome could contain just 4 numbers where each number is represented by 4 bits (the highest number therefore being 15.)

(b) Permutation Encoding

Permutation encoding can be used in scheduling problems, such as the traveling salesman problem or a task ordering problem. Every chromosome is a string of numbers, which represents number in a sequence. In the TSP each number would represent a city to be visited.



Figure 6 Example of Permutation Encoding

(c) Value Encoding

Direct value encoding can be used in problems where some complicated value, such as real numbers, is used and where binary encoding would not suffice. While value encoding is very good for some problems, it is often necessary to develop some specific crossover and mutation techniques for these chromosomes.

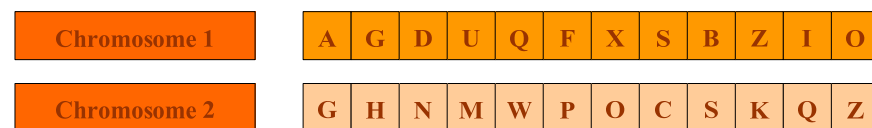


Figure 7 Example of Value Encoding

Figure 7 exhibits some examples of chromosomes encoded by value encoding. Gene A in chromosome 1 could represent a particular task and B could represent another. N in chromosome 2 could represent north and S could represent south. And thus, in this case, chromosome 2 represents a sequence of directions in which a person travels in a maze.

Selection

As mentioned earlier, chromosomes must be selected properly from the population to be parents for crossover. The problem is how to select these chromosomes properly. There are many selection methods. Examples are Roulette wheel selection, steady state selection.

(a) Roulette Wheel Selection

Simple reproduction allocates offspring strings using a roulette wheel with slots sized according to fitness. The probability of chromosomes to be selected from the population pool of chromosomes is proportional to their fitness. The fitter the chromosome, the greater chance it will be selected. However, it is not guaranteed that the fittest chromosome will survive in the next generation.

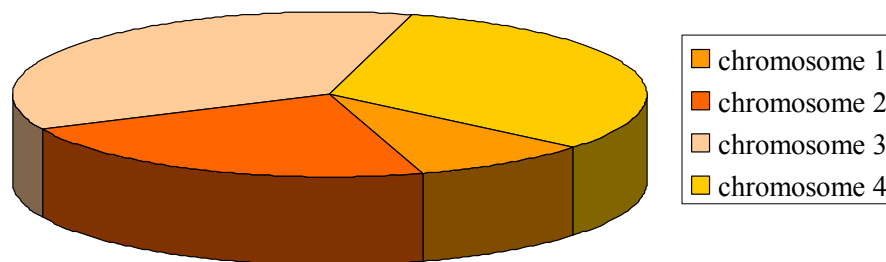


Figure 8 Graph of fitness

(b) Steady State Selection

In every generation, steady-state selection genetic algorithm performs selection in the following way. Only a few chromosomes with high fitness are selected for creating new offspring. Some chromosomes with low fitness are replaced by the new offspring. The rest of population will survive in the next generation.

(c) Rank Selection

The Roulette selection method of selection will have problems when the fitnesses of chromosomes are significantly different. For example, if the fitness of the fittest chromosome occupies 90% of the entire roulette wheel area then other chromosomes in the population pool will have an extremely small chance of being selected.

Rank selection at first ranks the chromosomes in the population pool from their fitness. For a rank selection of N chromosomes, the first N fittest chromosomes get selected.

Before:

Chromosome	Fitness
101001001100110	10
010010001100110	19
100011110110100	3

After:

Chromosome	Fitness
010010001100110	19
101001001100110	10
100011110110100	3

Figure 9 Example of Rank Selection (Before and After)

Crossover

After selection process, crossover operates on selected genes from parent chromosomes and creates new offspring. The simplest way to do that is to choose randomly a crossover point and copy everything before this point from the first parent and then copy everything after the crossover point from the other parent.

Crossover can be illustrated as follows:

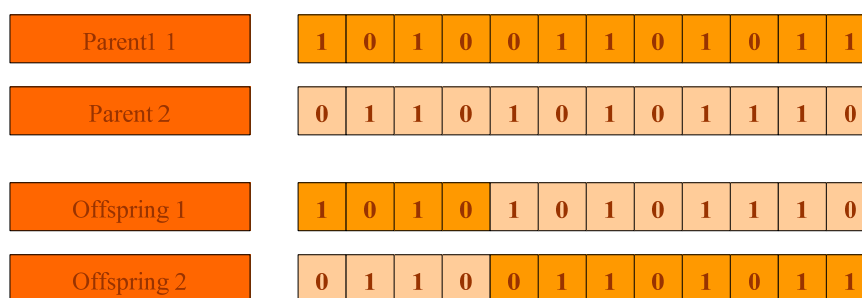


Figure 10 Example of Crossover

There are some other ways to perform crossover. For example we can select more than one crossover point. In this situation, crossover would be more

complicated and depend mainly on the encoding of chromosomes. However, specific crossover can help improve the performance of genetic algorithm.

Mutation

Mutation is actually a variation operator, which changes the information contained in the genome of a parent according to a given probability distribution. In the case of bit strings, this is realized by random negation (bit mutation, mutation rate) of single bits. Mutation is intended to prevent falling of all solutions in the population into a local optimum of the solved problem. Mutation operation randomly changes the offspring created by crossover. In case of binary encoding we can switch a few randomly chosen bits from 1 to 0 or from 0 to 1. Mutation can be then illustrated as follows:

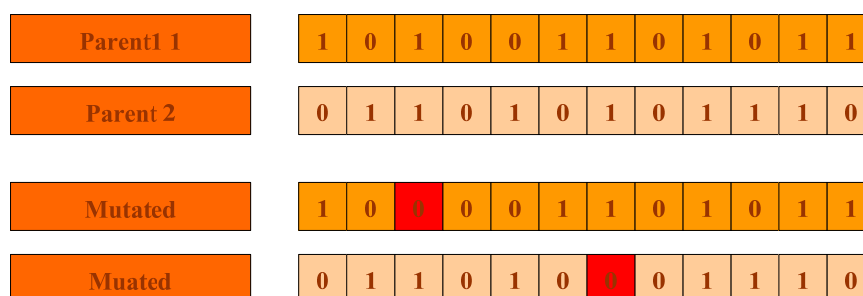


Figure 11 Example of Mutation

3. Antenna Arrays Theory

The radiation pattern of a single element is relatively wide and each element provides low value of directivity (gain). In many applications, it is necessary to design antennas with very directive characteristics (very high gains) to meet the demands of long distance communication. This can only be accomplished by increasing the electrical size of the antenna.

Enlarging the dimensions of single elements often leads to more directive characteristics. Another way to enlarge the dimensions of the antenna, without necessarily increasing the size of the individual elements, is to form an assembly of radiating elements in an electrical and geometrical configuration. This new antenna, formed by multi elements, is referred to as an array. In most cases, the elements of array are identical. This is not necessary, but it is often convenient, simpler, and more practical. The individual elements of an array may be of any form (wires, apertures, etc.).

The total field of the array is determined by vector addition of the field radiated by individual elements. This assumes that the current in each element is the same as that of isolated element (neglecting Coupling). This is usually not the case and depends on the separation between the elements. To provide very directive patterns, it is necessary that fields from the elements of the array interfere constructively (add) in the desired directions and interfere destructively (cancel each other) in the remaining space. Ideally this can be accomplished, but practically it is only approached. In an array of identical elements, there are at least five controls that can be used to shape the overall pattern of the antenna. These are:

1. the geometrical configuration of the overall array (linear, circular, rectangular, spherical)
2. the relative displacement between the elements
3. the excitation amplitude of individual elements
4. the excitation phase of the individual elements
5. the relative pattern of the individual elements

3.1. Array Factor of Planar

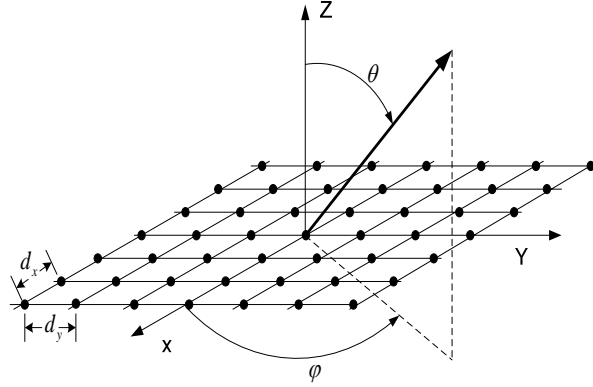


Figure 12 The Geometry for planar arrays of isotropic sources.

Array factor of 2-D (Planar) Array Expressed in term of $\vec{\Psi}$ or \hat{n} by setting $\beta_n = 0$, the array factor of an N-element antenna array contained in the x-y plane may be written as :

$$AF(\theta, \varphi) = AF(\vec{\Psi}) = \sum_{n=1}^N I_n e^{(j\vec{r} \cdot \vec{\Psi})} = \sum_{n=1}^N I_n e^{(j(\Psi_x x_n + \Psi_y y_n))} = AF(\Psi_x, \Psi_y) \quad (3.1.1)$$

$$= AF(\hat{n}) = \sum_{n=1}^N I_n e^{(jk\hat{r} \cdot \hat{n})} = \sum_{n=1}^N I_n e^{(jk(n_x x_n + n_y y_n))} = AF(n_x, n_y) \quad (3.1.2)$$

Where $\vec{\Psi}$ is a vector whose component along the x-axes and y-axes are Ψ_x and Ψ_y , respectively, and \hat{n} is a unit vector whose component along x-axes and y-axes are n_x and n_y , respectively.

$$AF(\vec{\Psi}) = AF(\hat{n}) = \sum_{n=1}^N I_n e^{(j\vec{r} \cdot \vec{\Psi})} = AF(\hat{n}) = \sum_{n=1}^N I_n e^{(j\hat{n} \cdot \vec{\Psi})} \quad (3.1.3)$$

The function has the following properties:

1. The visible region is $|\hat{n}_x + \hat{n}_y| \leq |\hat{n}| = 1$ or $|\vec{\Psi}_x + \vec{\Psi}_y| \leq |\vec{\Psi}| = k$
2. The visible region of the function

$$AF(\vec{\Psi} - \vec{\Psi}_0) = AF(\hat{n} - \hat{n}_0) = \sum_{n=1}^N I_n e^{(j\vec{r} \cdot (\vec{\Psi} - \vec{\Psi}_0))} = AF(\hat{n}) = \sum_{n=1}^N I_n e^{(jk\hat{r}_n \cdot (\hat{n} - \hat{n}_0))}$$

$$\left[(\hat{n}_x - \hat{n}_{x_0}) + (\hat{n}_y - \hat{n}_{y_0}) \right] \leq |\hat{n} - \hat{n}_0| = 1 \text{ or } \left[(\vec{\Psi}_x - \vec{\Psi}_{x_0}) + (\vec{\Psi}_y - \vec{\Psi}_{y_0}) \right] \leq |\vec{\Psi}| = k$$

3. $AF(\bar{\Psi}) = \overline{AF(-\bar{\Psi})}$ and $AF(\hat{n}) = \overline{AF(-\hat{n})}$
4. $AF_1(a\hat{n}) = AF_2(\hat{n})$ where a is a scalar quantity and $AF_1(\hat{n})$ and $AF_2(\hat{n})$ are the arrays factors in term of \hat{n} with the minimum spacing $d_{\min} = d_1$ and $d_2 = ad_1$, respectively.

Where I_n represents the excitation amplitude of the n th element to be controlled and represents the angle of maximum radiation. In this thesis, excitation amplitude of each element is changed by using genetic algorithms. In this case, fitness function is the lowest of sidelobe.

3.2. The mainlobe and sidelobes

According to the beampattern in Figure 13, the highest peak in the mainlobe while the smaller peaks are Sidelobe. The beampattern may be interpreted as the spatial filter response of an array. Thus the mainline is similar to the passband in a spatial bandpass filter, which only passes signals in these directions. Similar to filter design in digital signal processing, we would like the beam to approach the delta pulse or equally an infinitely thin beam. But from array processing theory, this is impossible using an array with finite spatial extension. The location of mainlobe peak tells in which direction we get maximum response with the array. Another measure used to characterize the mainlobe is the mainlobe width or the beamwidth. Here we define it to be the full width of the mainlobe at 6dB below the mainlobe peak on the

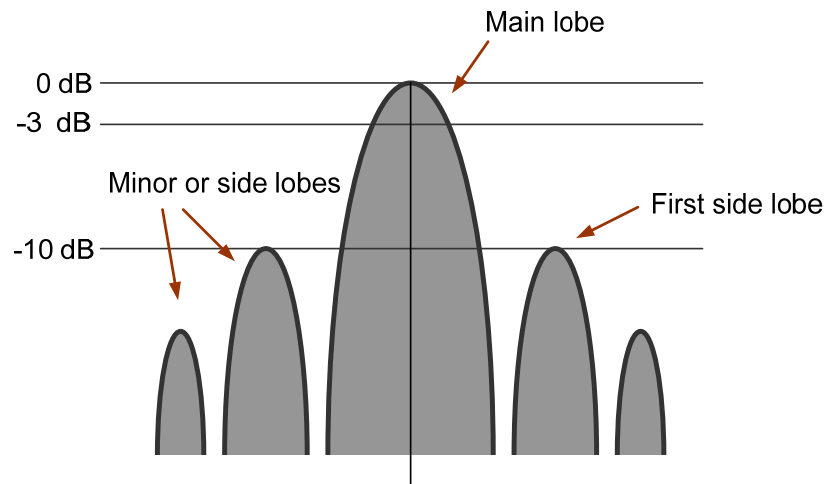


Figure 13 Linear plot of power pattern and its associated lobes.

Beampattern From the angular array pattern, we can measure at which angle 2ϕ the mainlobe has dropped 6dB. The beamwidth is then ϕ for consistency and usually measured in degrees. The Sidelobe in the beampattern is equal to the stopband in a bandpass filter. As is known from window filter design, the Sidelobe can not be completely rejected using a finite aperture. But the Sidelobe can be suppressed a certain degree by adjusting the amplitude weights and elements positions. The sidelobe region or equally the stopband, is conveniently defined as the area in the plane outside the first zero crossing of the mainlobe. The sidelobe level is used as a measure on the height of the highest sidelobe peak in the sidelobe region and usually given in dB. The height of the highest sidelobe relative to the mainlobe measures an array's ability to reject unwanted noise and signals, and focus on particular propagating signals.

MATERIAL AND METHODS

Material

1. MATLAB™ (Matrix Laboratory) version 6.5
2. Personal computer (AMD Athlon™ XP 3800 Dual Core+ 1.67 GHz processor 1GB of RAM) for testing the proposed Matlab code.

Method

Our primary purpose is to synthesize an antenna with low sidelobes. To achieve the goal we use the concept of genetic algorithm and fractal geometry. We develop two Matlab codes to synthesize antenna arrays with low sidelobes in two approaches as follow:

1.1. Generate the Peano-Gosper fractal array for the stage of growth 3. Generate an initial population of chromosomes representing the relative current excitation of the stage 3 Peano-Gosper fractal array. Then, apply genetic algorithm for optimizing the stage 3 Peano-Gosper fractal array with low sidelobes

1.2. Generate the Peano-Gosper fractal array generator (the Peano-Gosper fractal array for the stage of growth 1). Generate an initial population of chromosomes representing the relative current excitation of the Peano-Gosper fractal array generator. Then, apply genetic algorithm for optimizing the stage 3 Peano-Gosper fractal array with low sidelobes

1. Procedure to construct the Peano-Gosper Curve

1. Start with the same initiator as the Peano curve shown in Figure 5.1



Figure14 The Peano-Gosper curve initiator

2. At Stage 1, replace the initiator with generator shown in figure 5.2

3. At Stage 2, turn the generator counterclockwise as shown in Figure 5.2 until the link between both ends is aligned in the same direction as of each line segment of the generator(s) in the previous stage. Scale the generator until the size of the links at both ends is the same as that of each line segment of generator. Replace each line segment of the generated curve at the previous stage with an appropriately scaled version of the generator.

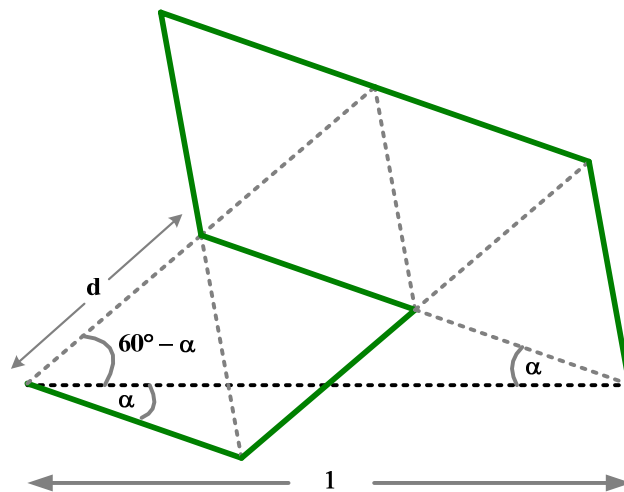


Figure15 The Peano-Gosper curve generator

4. Repeat step 3 for further stages (stage 3)

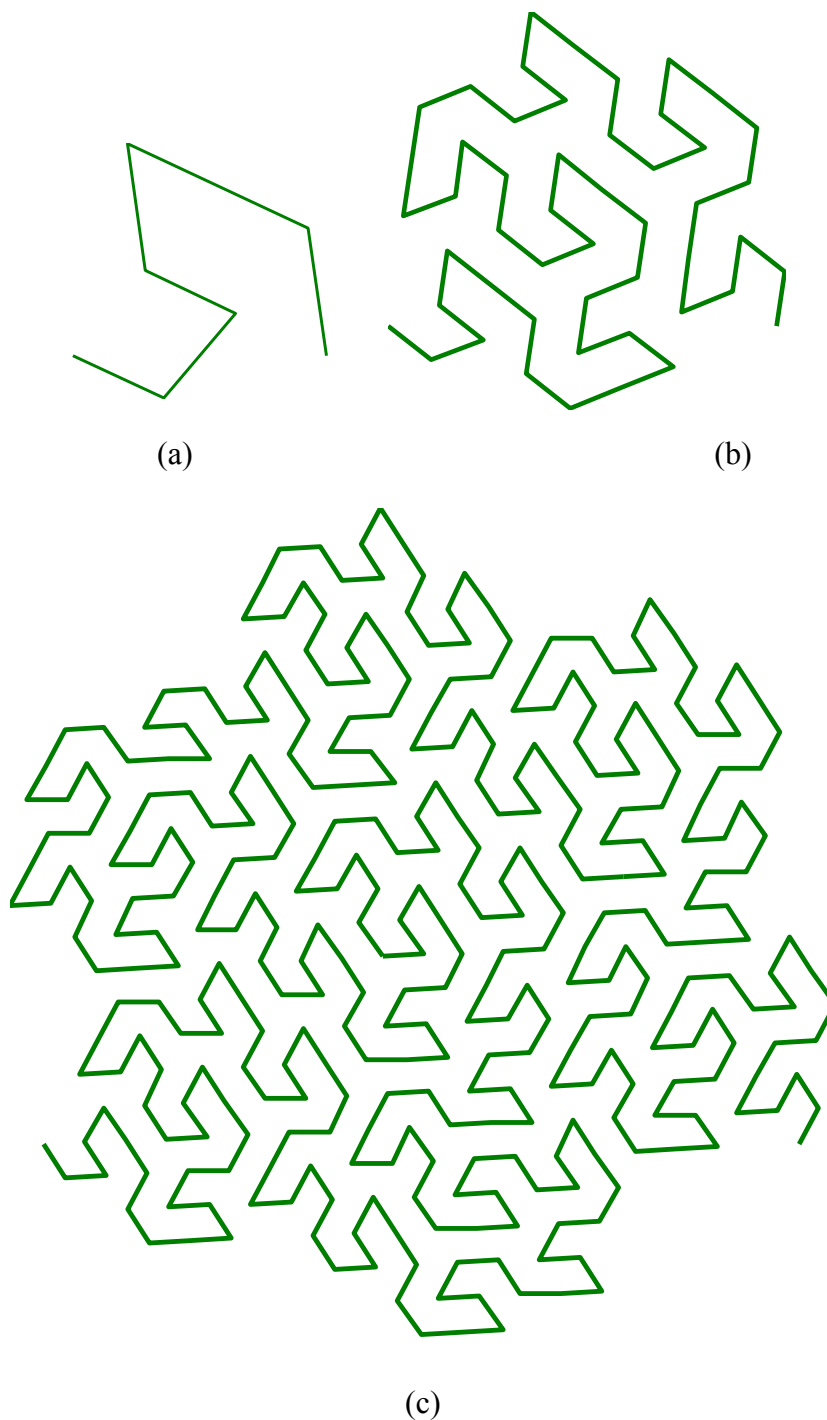


Figure16 The first three stages in the construction of self-avoiding Peano-Gosper curve. The initiator is shown as the dashed line superimposed on the stage 1 generator. The generator (unscaled) is shown again in (b) as the dashed curve superimposed on the stage 2 Peano-gosper curve

2. Case study

In this work, the objective of this research is to synthesize antenna arrays using the concept of genetic algorithm and fractal geometry. We apply fractal geometry to strategically place antenna elements on the Peano-gosper fractal array and genetic algorithm to synthesize the antenna array optimized by reducing overall sidelobe level.

For approach 1, we represent a relative current excitation on 344 elements of the stage 3 Peano-Gosper fractal array by a 344 binary (decimal) gene chromosome whereas for approach 2, we code a relative current excitation on 8 elements of the Peano-Gosper fractal array generator.

For each generation (iteration), for both approaches, we generate 64 chromosomes in the population for each individual generation. Rank selection is chosen for the selection process; the first 50% of the fittest chromosomes are selected. The 50% less fit chromosomes die off. All selected chromosomes are grouped in couples. Hence, the first 50% of the fittest chromosomes consists of 32 pairs of chromosomes (32 couple of parents). A couple of parents consists of two consecutive ranked chromosomes. In the crossover process, the crossover point is placed at the midpoint of each individual chromosome. Each couple of parents creates 2 offspring. For mutation, 10% of the population is randomly selected. For each chromosome, randomly select a gene to mutate. The genetic algorithm iterates for 100 generations (iterations).

Case1. The genetically optimized stage3 Peano-Gosper curve

In this case, the parameters for each individual case are selected as follow:

1. Minimum Spacing = 0.5λ and Maximum Current Excitation = 1
2. Minimum Spacing = 1λ and Maximum Current Excitation = 1
3. Minimum Spacing = 0.5λ and Maximum Current Excitation = 10
4. Minimum Spacing = 1λ and Maximum Current Excitation = 10

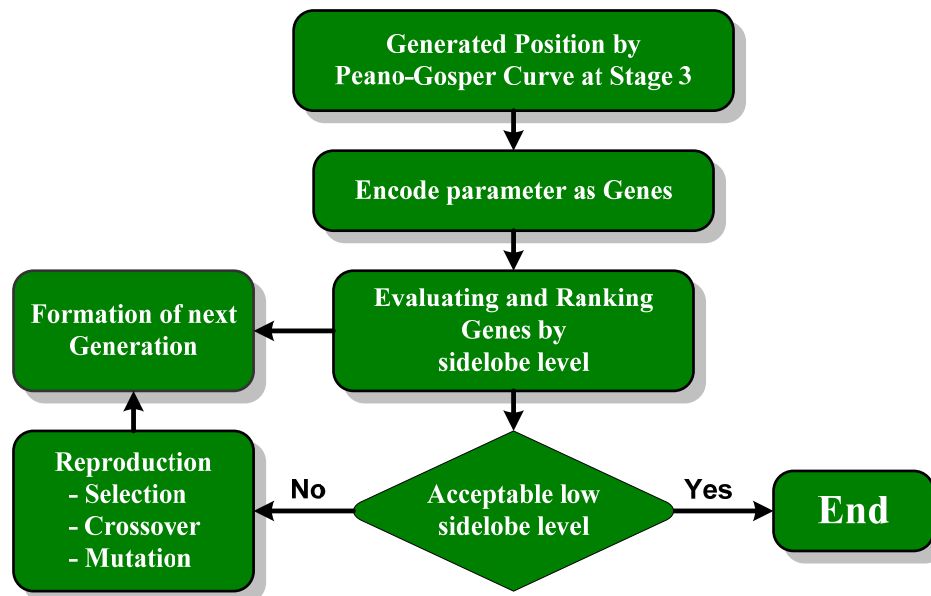


Figure17 Flow Chart of Methodologies case1

Case 2 The genetically optimized stage1 Peano-Gosper curve and create higher order stage arrays (stage 3).

In this case, the parameters for each individual case are selected as follow:

1. Minimum Spacing = 0.5λ and Maximum Current Excitation = 1
2. Minimum Spacing = 1λ and Maximum Current Excitation = 1
3. Minimum Spacing = 0.5λ and Maximum Current Excitation = 10
4. Minimum Spacing = 1λ and Maximum Current Excitation = 10

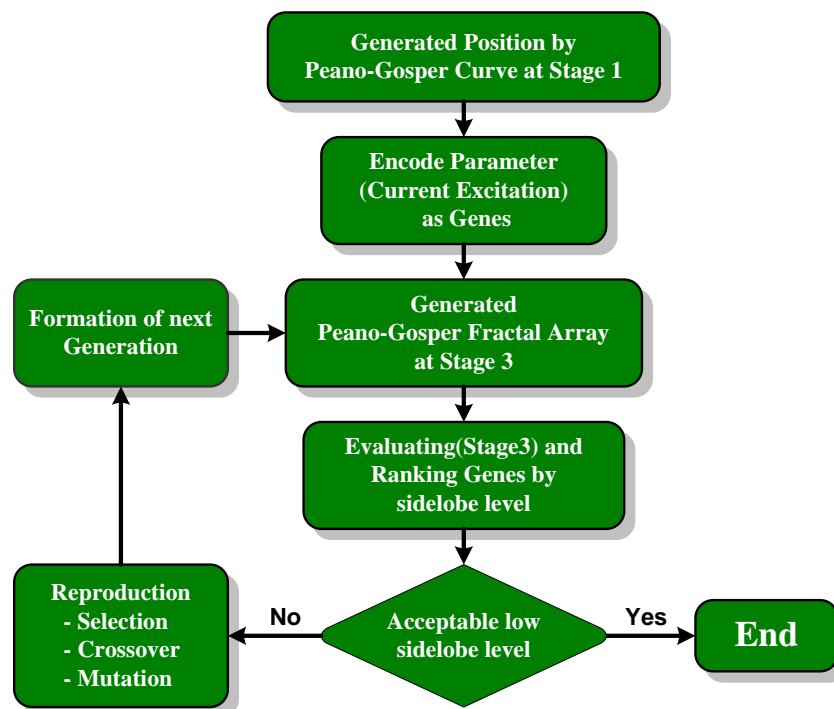


Figure18 Flow Chart of Methodologies for case 2

RESULT AND DISCUSSION

1. Peano-Gosper Fractal Arrays Synthesis Using Genetic Algorithms

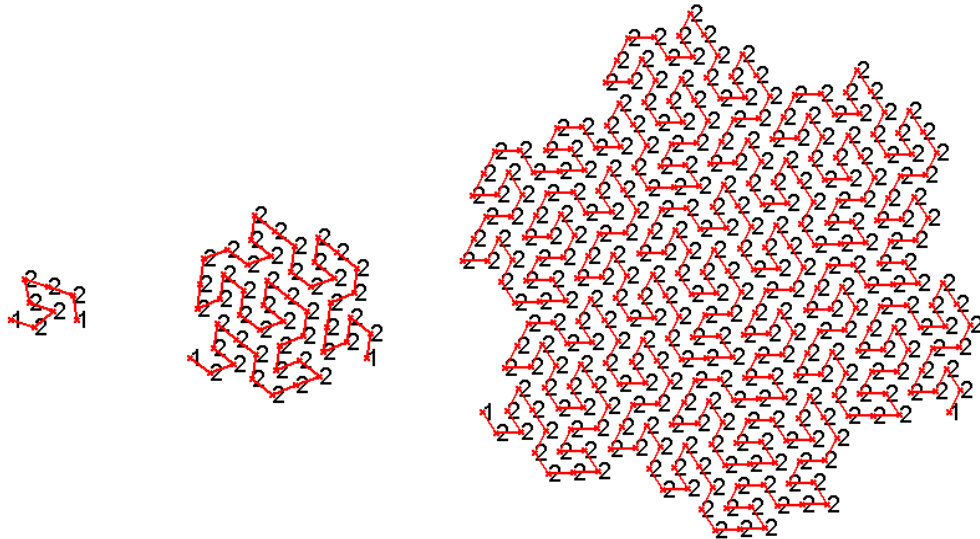


Figure19 The Peano-Gosper fractal arrays configurations and their relative current excitation for the stages of growth 1, 2 and 3, respectively

Simulation results of the Peano-Gosper fractal arrays subjected to different parameters are presented as follow:

1.1 The genetically optimized stage3 Peano-Gosper fractal array

a. Minimum distance equal $\lambda/2$ and Maximum of current excitation equals 1

Consider the genetically optimized stage 3 Peano-Gosper fractal array with minimum spacing of $\lambda/2$ and maximum current excitation of 1. Figure 20 exhibits the Peano-Gosper fractal array for the stages of growth 1, 2 and 3, respectively. Figure 21 exhibits the sidelobe level of the Peano-Gosper fractal arrays for the stage of growth 3 versus generation. In addition, Figure 22 shows the plot of the normalized stage 3 Peano-Gosper fractal array, genetically optimized array factor versus (a) ϕ for (a) $\theta = 90^\circ$ and (b) θ for $\phi = 90^\circ$ where minimum distance equals $\lambda/2$ and maximum current excitation equals one.

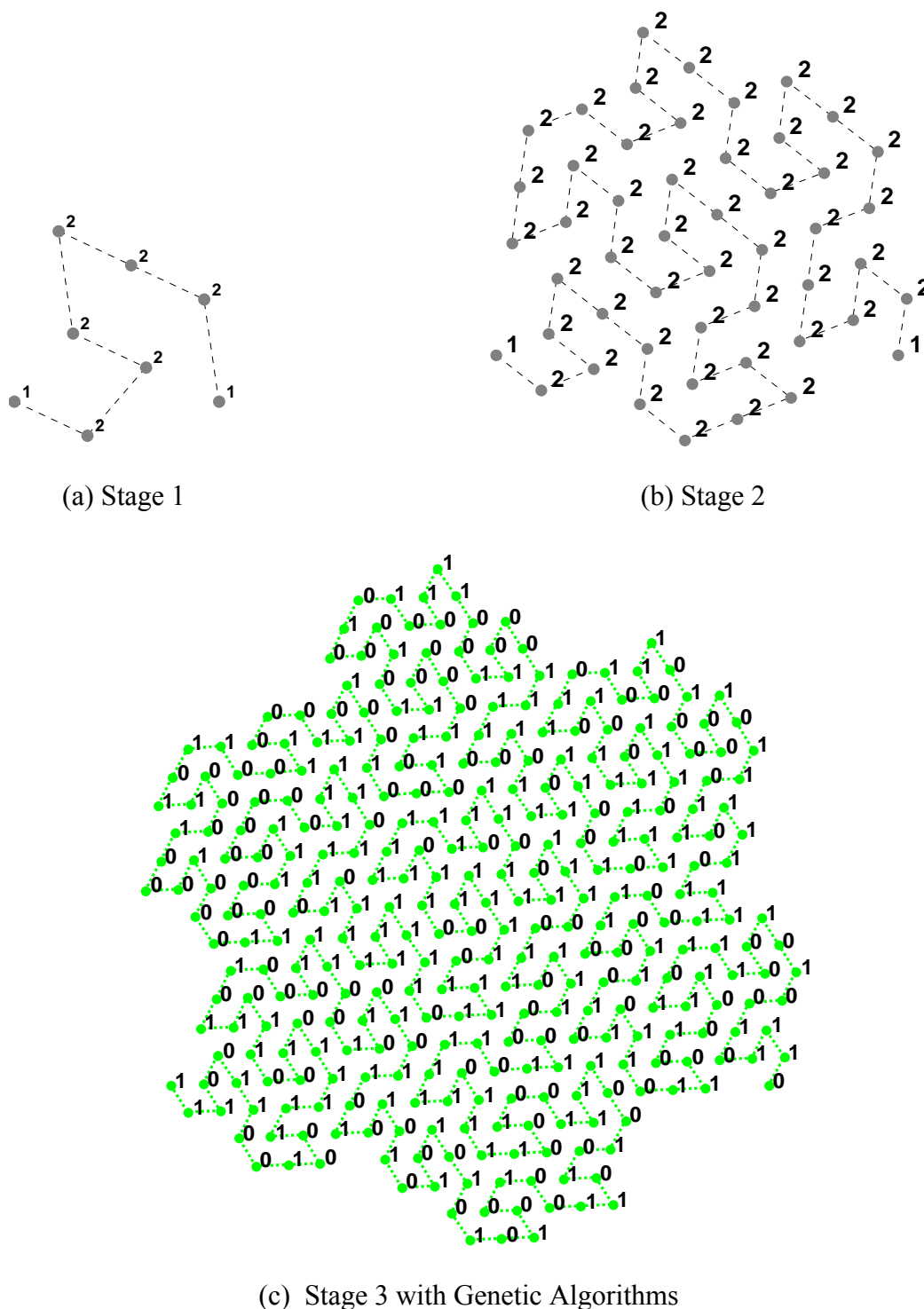


Figure 20 Element location for the (a) stage 1, (b) stage 2, and (c) stage 3 Peano-Gosper fractal arrays. A uniform spacing of d_{\min} is assumed between consecutive arrays elements which is the same for each stage, minimum spacing is $\lambda/2$, maximum current excitation is one.

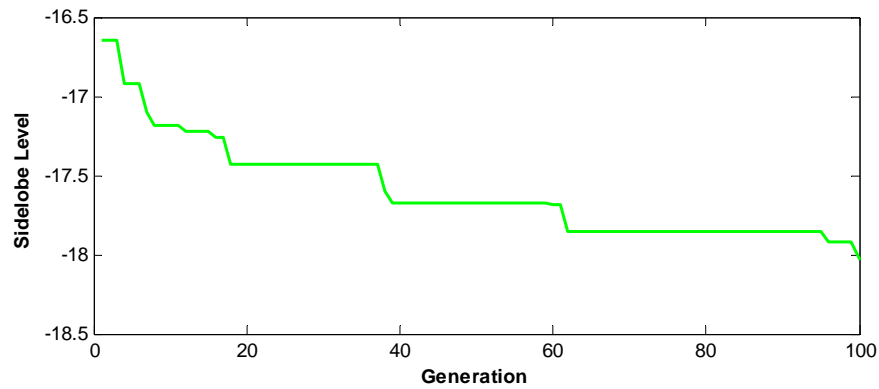
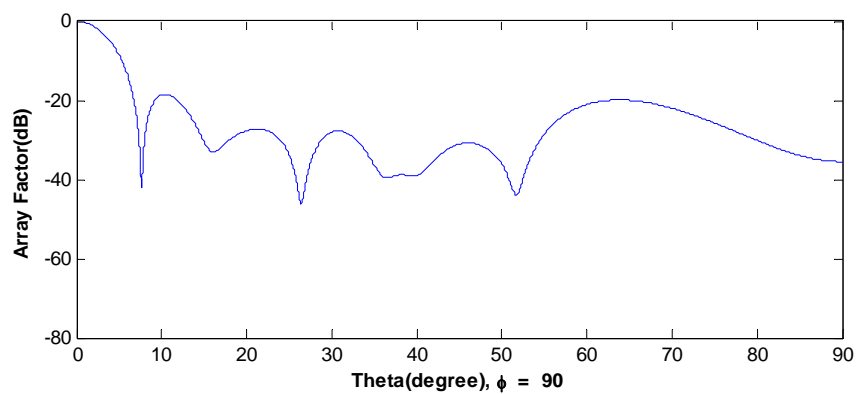
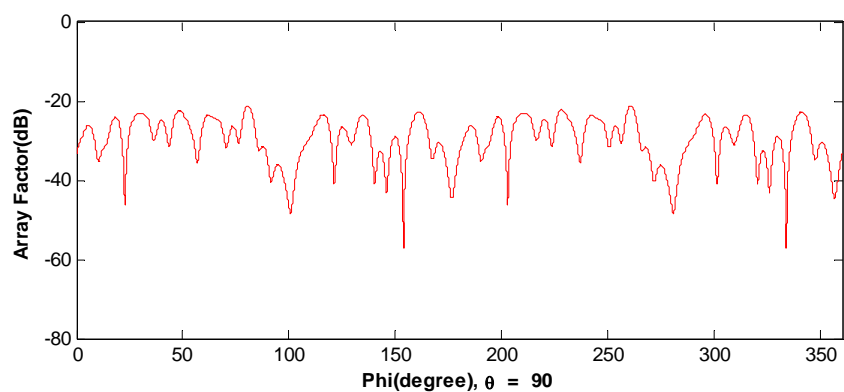


Figure 21 Evolution diagram of Genetically Optimized a Stage3: Peano-Gosper Fractal Array, minimum spacing is $\lambda/2$, maximum current excitation is one

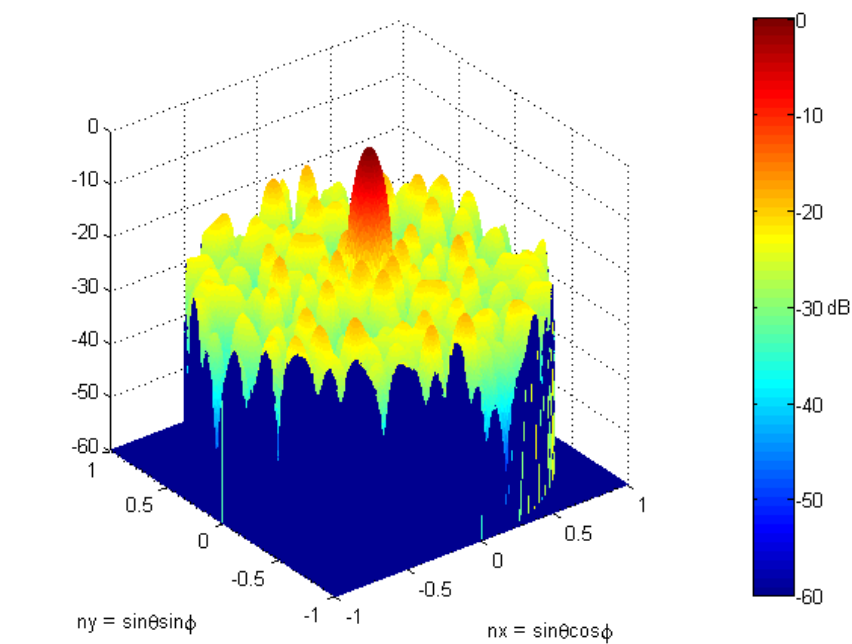


(a)

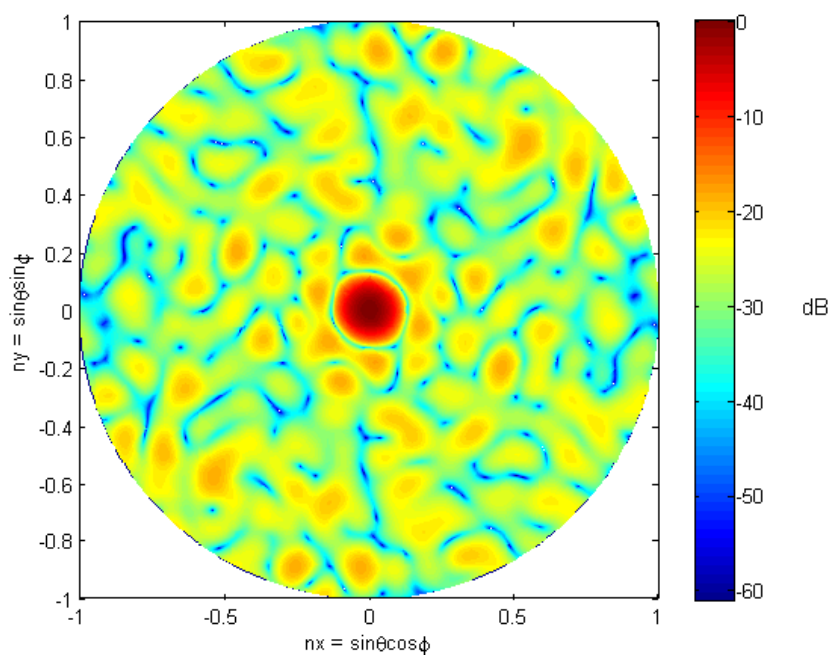


(b)

Figure 22 Plot of the normalized stage 3 Peano-Gosper fractal array, genetically optimized array factor versus (a) ϕ for $\theta = 90^\circ$ and (b) θ for $\phi = 90^\circ$ where minimum distance equals $\lambda/2$ and maximum current excitation equal one



(a)



(b)

Figure 23 The normalized radiation pattern in dB for stage 3 of Peano-Gosper fractal array from Figure 20c with a minimum spacing is λ , maximum current excitation is one and main beam steered to $\theta = 0$ degrees and $\phi = 90^\circ$ degrees. (a) Radiation Pattern, and (b) Top View

b. Minimum distance equal λ and Maximum of current excitation equal 10

Consider the genetically optimized stage 3 Peano-Gosper fractal array with minimum spacing of λ and maximum current excitation of 10. Figure 24 exhibits the Peano-Gosper fractal array for the stages of growth 1, 2 and 3, respectively. Figure 25 exhibits the sidelobe level of the Peano-Gosper fractal arrays for the stage of growth 3 versus generation. In addition, Figure 26 shows the plot of the normalized stage 3 Peano-Gosper fractal array, genetically optimized array factor versus (a) ϕ for (a) $\theta = 90^\circ$ and (b) θ for $\phi = 90^\circ$ where minimum distance equals λ and maximum current excitation equals ten.

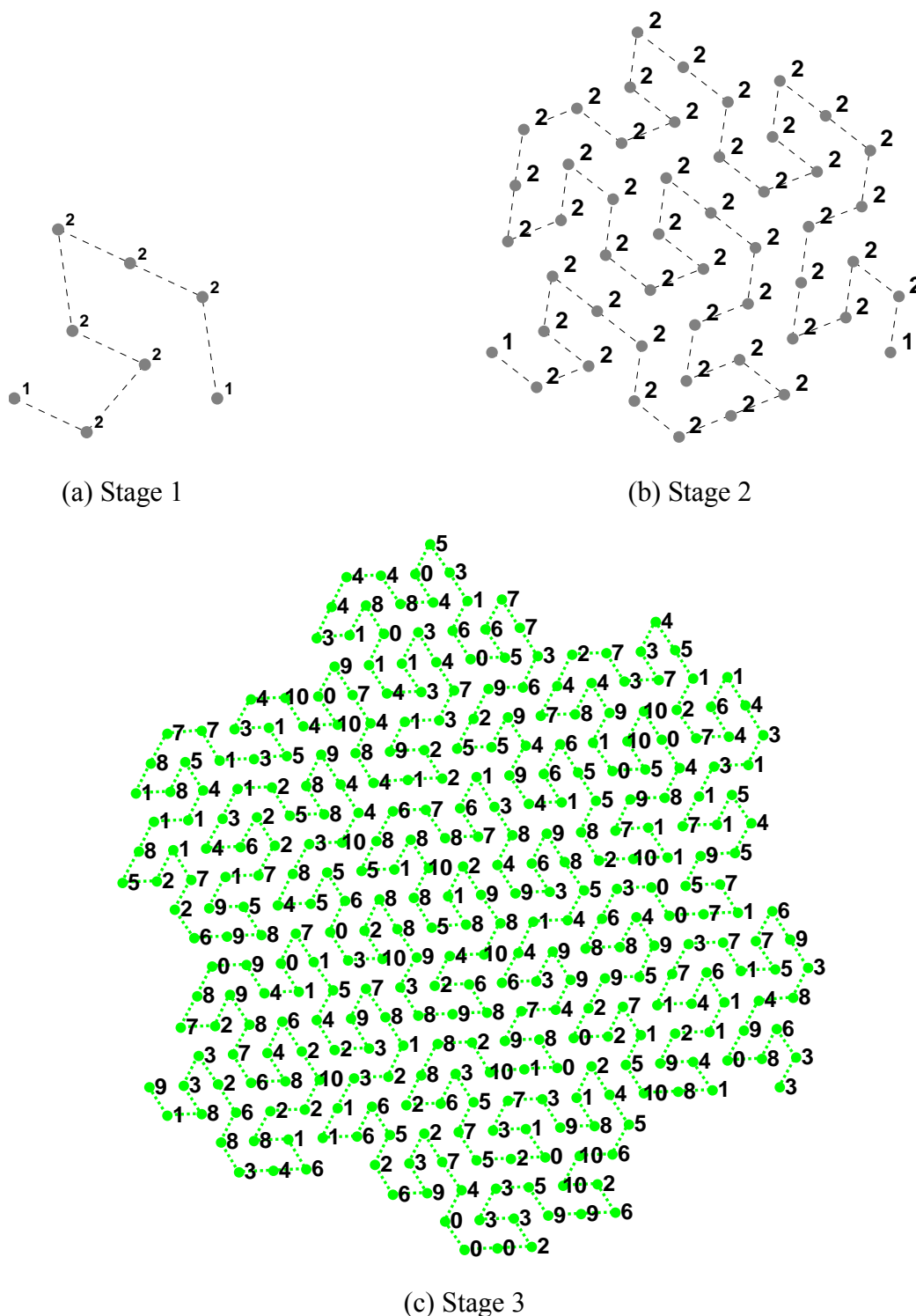


Figure 24 Element location for the (a) stage 1, (b) stage 2, and (c) stage 3 Peano-Gosper fractal arrays. A uniform spacing of d_{\min} is assumed between consecutive arrays elements which is the same for each stage, minimum spacing is $\lambda/2$, maximum current excitation is ten.

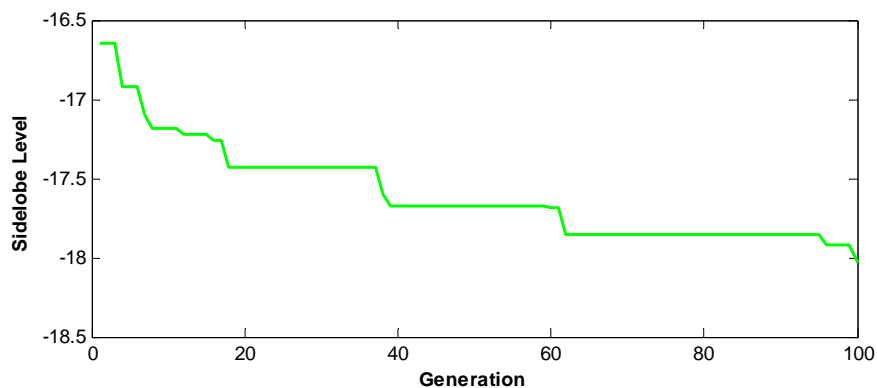


Figure 25 Evolution diagram of Genetically Optimized a Stage3: Peano-Gosper Fractal Array, minimum spacing is $\lambda/2$, maximum current excitation is ten.

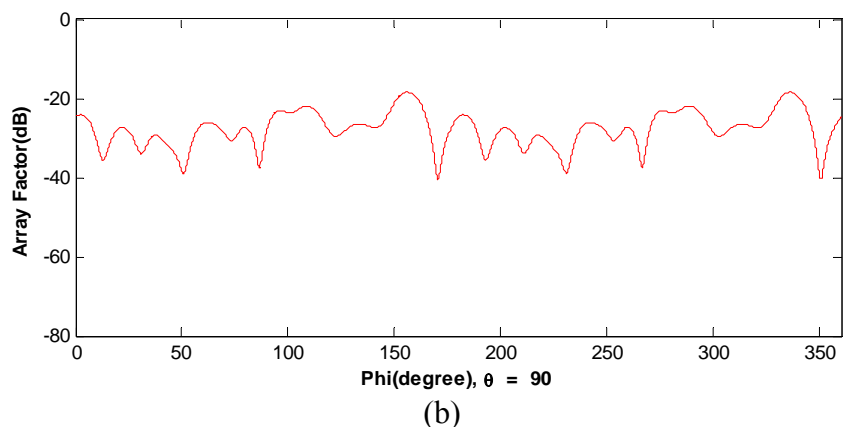
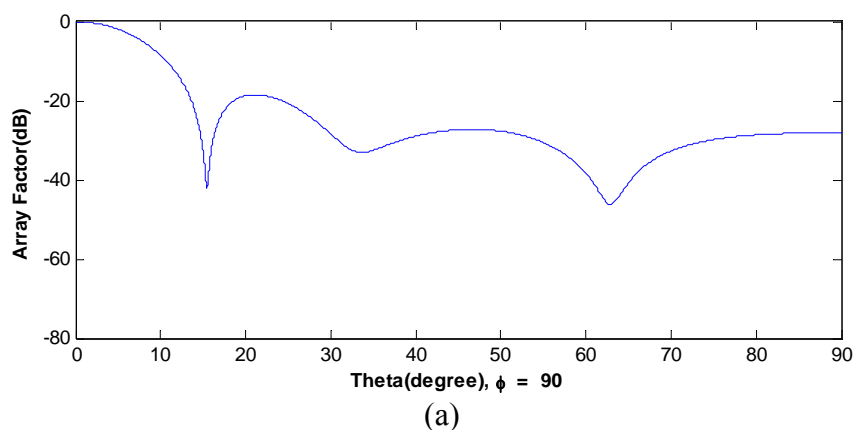
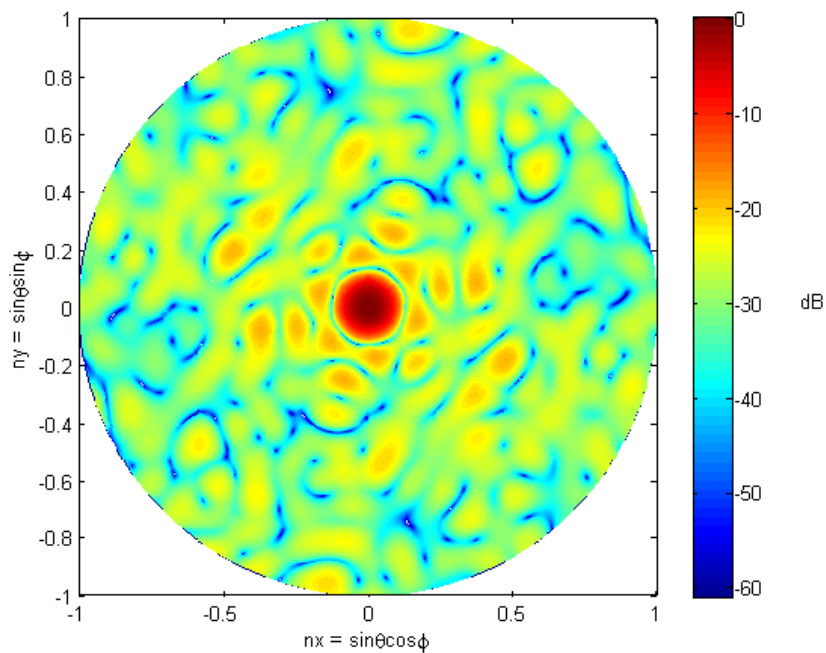
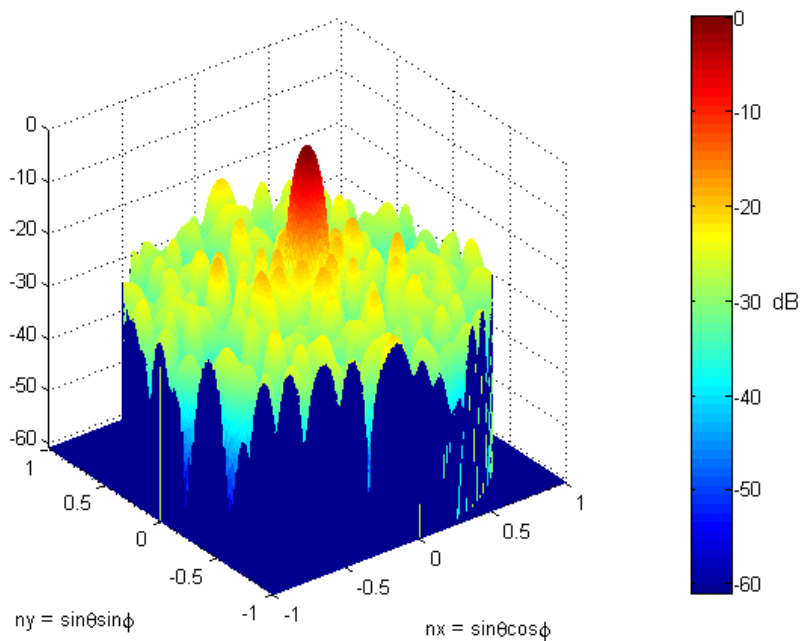


Figure 26 Plot of the normalized stage 3 Peano-Gosper fractal array, genetically optimized array factor versus (a) ϕ for $\theta = 90^\circ$ and (b) θ for $\phi = 90^\circ$ where minimum distance equal $\lambda/2$ and maximum current excitation equal ten.



(a)



(b)

Figure 27 The normalized radiation pattern in dB for stage 3 of Peano-Gosper fractal array from Figure 24c with a minimum spacing is $\lambda/2$, maximum current excitation is ten and main beam steered to $\theta = 0$ degrees and $\phi = 90^\circ$ degrees.(a) Radiation Pattern, and (b) Top view.

c. Minimum distance equal λ and Maximum of current excitation equal one

Consider the genetically optimized stage 3 Peano-Gosper fractal array with minimum spacing of λ and maximum current excitation of 1. Figure 28 exhibits the Peano-Gosper fractal array for the stages of growth 1, 2 and 3, respectively. Figure 29 exhibits the sidelobe level of the Peano-Gosper fractal arrays for the stage of growth 3 versus generation. In addition, Figure 30 shows the plot of the normalized stage 3 Peano-Gosper fractal array, genetically optimized array factor versus (a) ϕ for (a) $\theta = 90^\circ$ and (b) θ for $\phi = 90^\circ$ where minimum distance equals λ and maximum current excitation equals one.

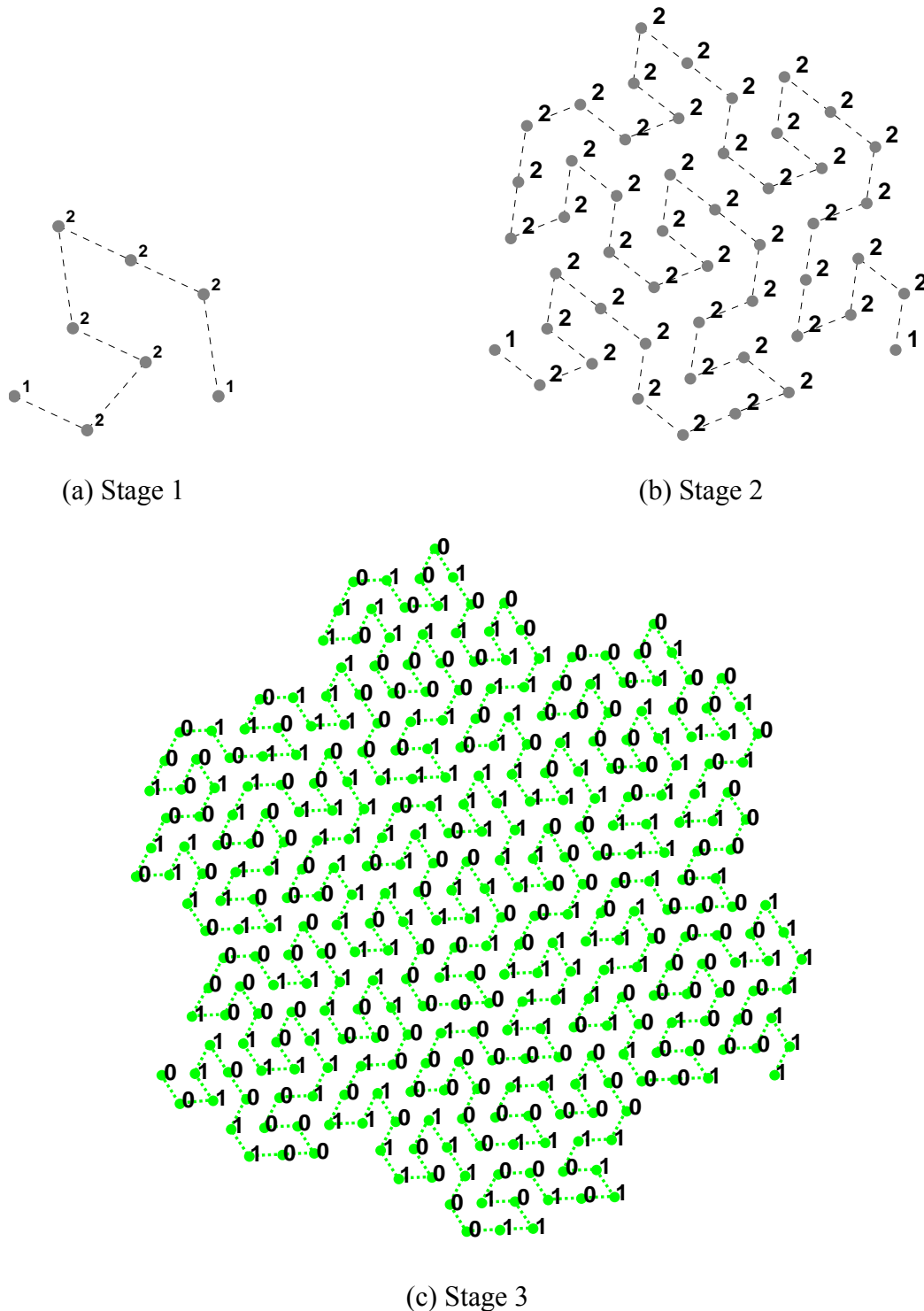


Figure 28 Element location for the (a) stage 1, (b) stage 2, and (c) stage 3 Peano-Gosper fractal arrays. A uniform spacing of d_{\min} is assumed between consecutive arrays elements which is the same for each stage, minimum spacing is λ , maximum current excitation is one.

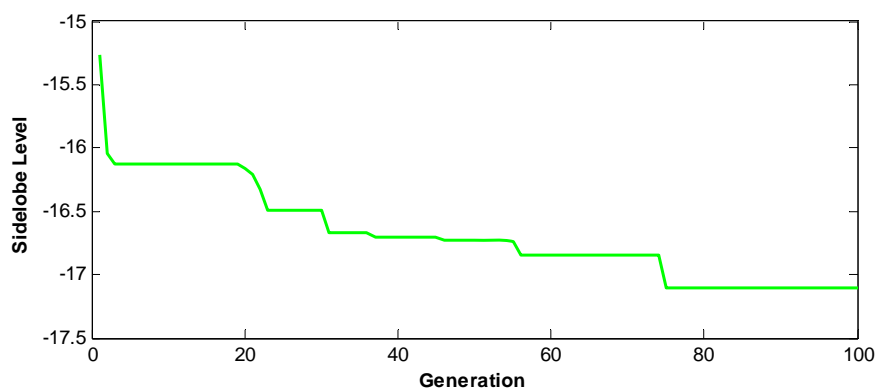
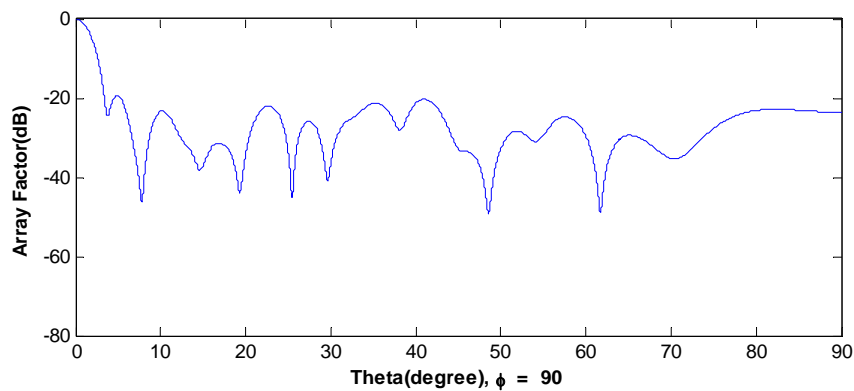
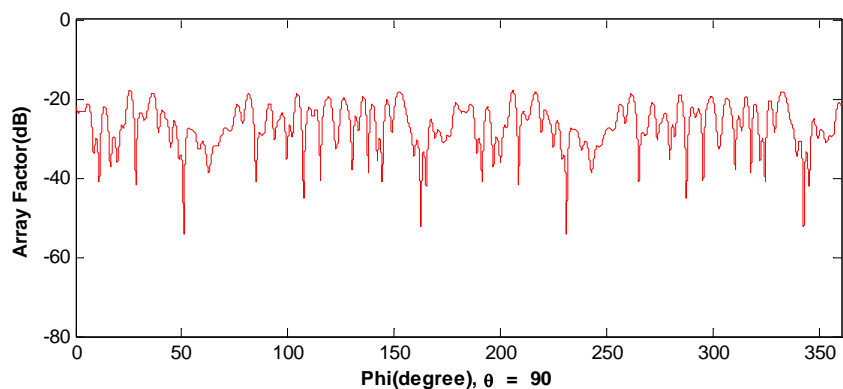


Figure 29 Evolution diagram of Genetically Optimized a Stage3: Peano-Gosper Fractal Array, minimum spacing is λ , maximum current excitation is one.

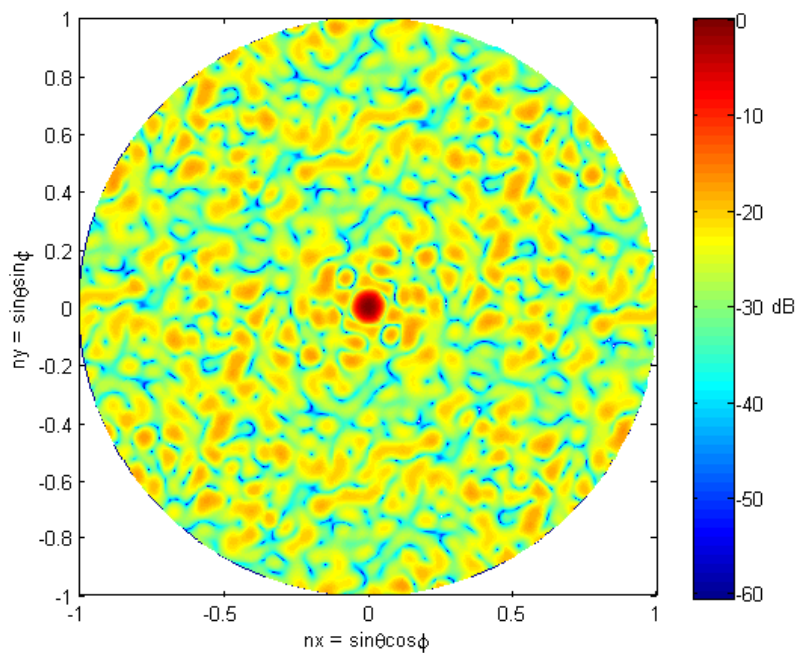


(a)

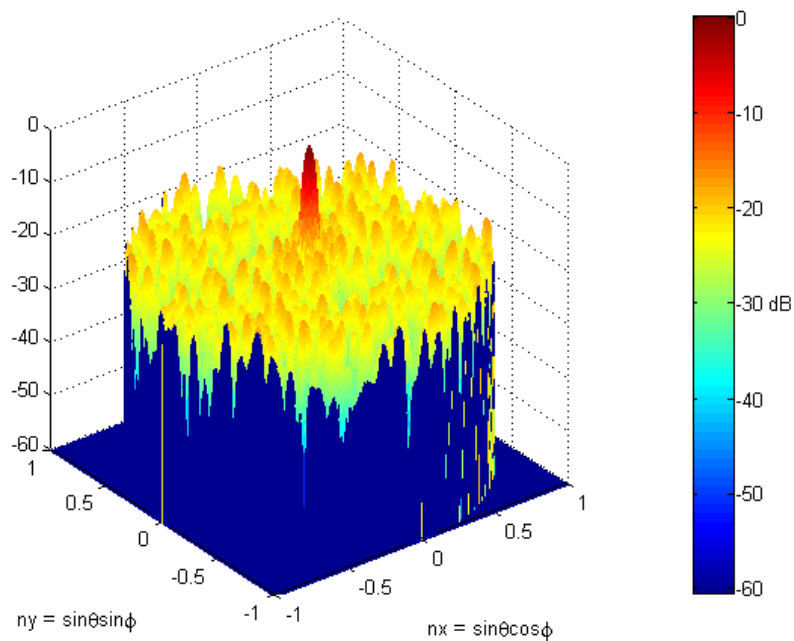


(b)

Figure 30 Plot of the normalized stage 3 Peano-Gosper fractal array, genetically optimized array factor versus (a) ϕ for $\theta = 90^\circ$ and (b) θ for $\phi = 90^\circ$ where minimum distance equal λ and maximum current excitation equal one.



(a)



(b)

Figure 31 The normalized radiation pattern in dB for stage 3 of Peano-Gosper fractal array from Figure 28c with a minimum spacing is λ , maximum current excitation is one and main beam steered to $\theta = 0$ degrees and $\phi = 90^\circ$ degrees. (a) Radiation Pattern, and (b) Top View

d. Minimum distance equal λ and Maximum of current excitation equal ten

Consider the genetically optimized stage 3 Peano-Gosper fractal array with minimum spacing of λ and maximum current excitation of 10. Figure 32 exhibits the Peano-Gosper fractal array for the stages of growth 1, 2 and 3, respectively. Figure 33 exhibits the sidelobe level of the Peano-Gosper fractal arrays for the stage of growth 3 versus generation. In addition, Figure 34 shows the plot of the normalized stage 3 Peano-Gosper fractal array, genetically optimized array factor versus (a) ϕ for (a) $\theta = 90^\circ$ and (b) θ for $\phi = 90^\circ$ where minimum distance equals λ and maximum current excitation equals ten.

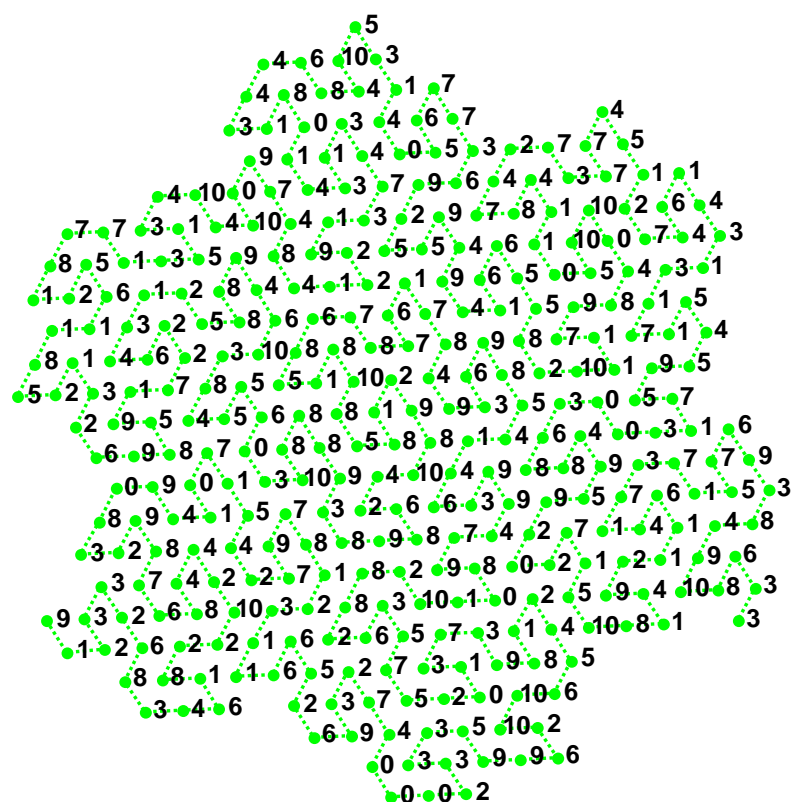
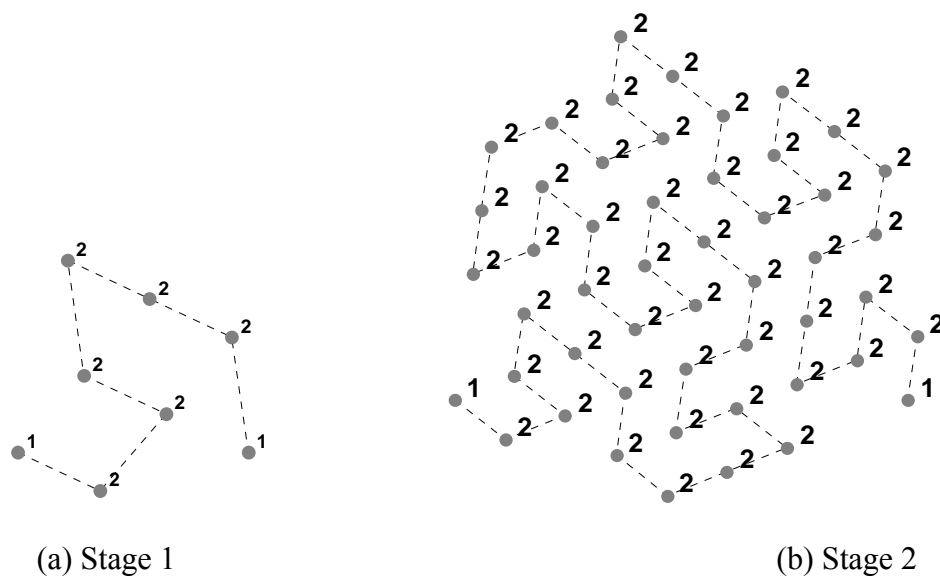


Figure 32 Element location for the (a) stage 1, (b) stage 2, and (c) stage 3 Peano-Gosper fractal arrays. A uniform spacing of d_{\min} is assumed between consecutive arrays elements which is the same for each stage, minimum spacing is λ , maximum current excitation is ten.

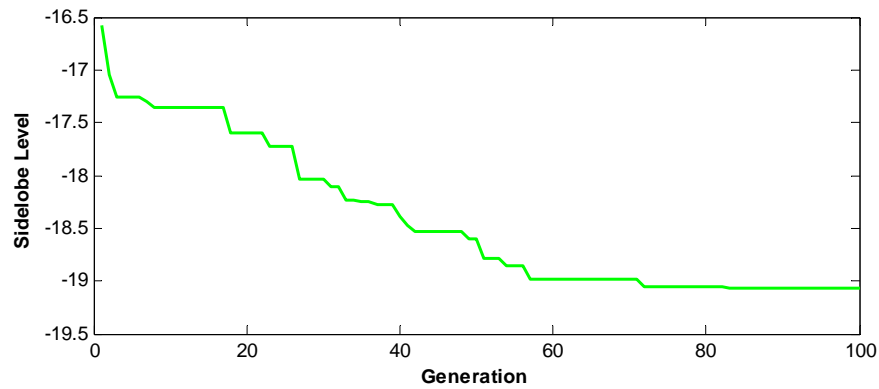
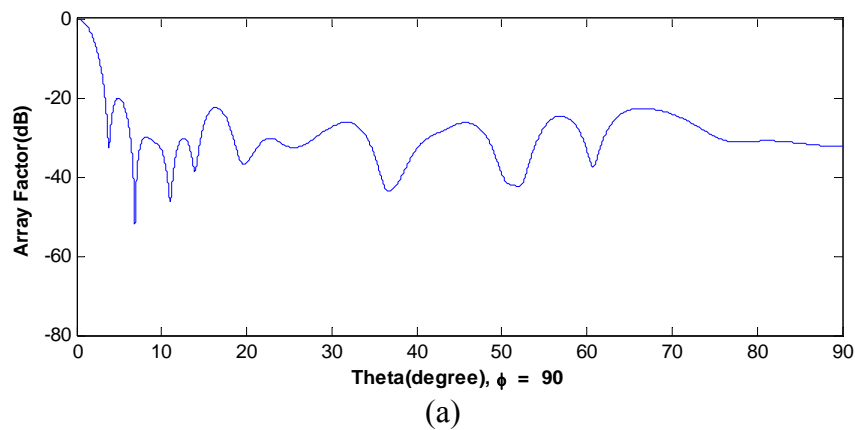
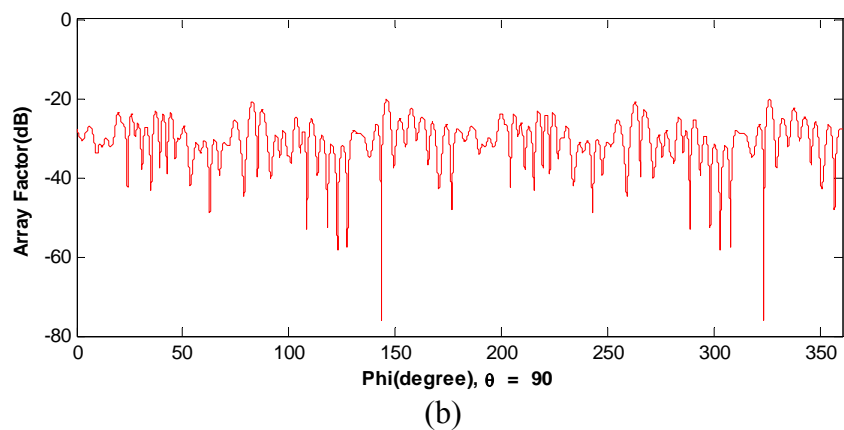


Figure 33 Evolution diagram of Genetically Optimized a Stage3: Peano-Gosper Fractal Array, minimum spacing is λ , maximum current excitation is ten.

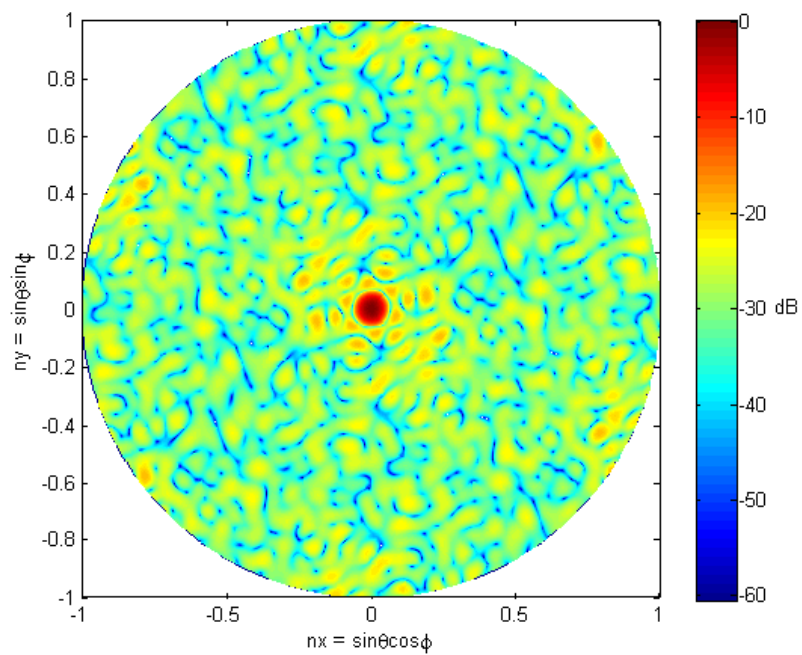


(a)

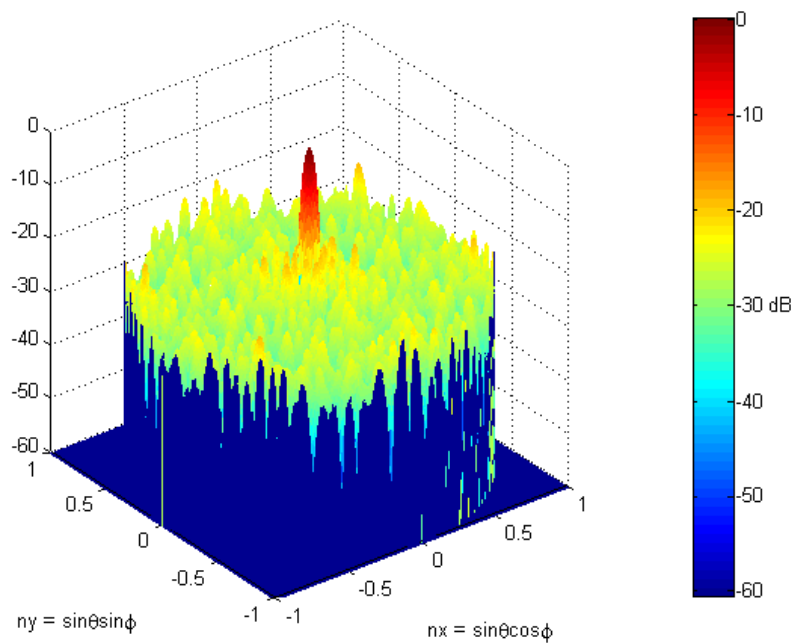


(b)

Figure 34 Plot of the normalized stage 3 Peano-Gosper fractal array, genetically optimized array factor versus (a) ϕ for $\theta = 90^\circ$ and (b) θ for $\phi = 90^\circ$ where minimum distance equal λ and maximum current excitation equal ten.



(a)



(b)

Figure 35 The normalized radiation pattern in dB for stage 3 of Peano-Gosper fractal array from Figure 32c with a minimum spacing is λ , maximum current excitation is ten and main beam steered to $\theta = 0$ degrees and $\phi = 90^\circ$ degrees. (a) Radiation Pattern, and (b) Top View.

1.2. The genetically optimized stage1 Peano-Gosper curve and create higher order stage arrays (stage 3).

a. Minimum distance equal $\lambda/2$ and Maximum of current excitation equal one

Consider the genetically optimized stage 1 Peano-Gosper fractal array and create higher order stage arrays (stage 3) with minimum spacing of $\lambda/2$ and maximum current excitation of 1. Figure 36 exhibits the Peano-Gosper fractal array for the stages of growth 1, 2 and 3, respectively. Figure 37 exhibits the sidelobe level of the Peano-Gosper fractal arrays for the stage of growth 3 versus generation. In addition, Figure 38 shows the plot of the normalized stage 3 Peano-Gosper fractal array, genetically optimized array factor versus (a) ϕ for (a) $\theta = 90^\circ$ and (b) θ for $\phi = 90^\circ$ where minimum distance equals $\lambda/2$ and maximum current excitation equals one.

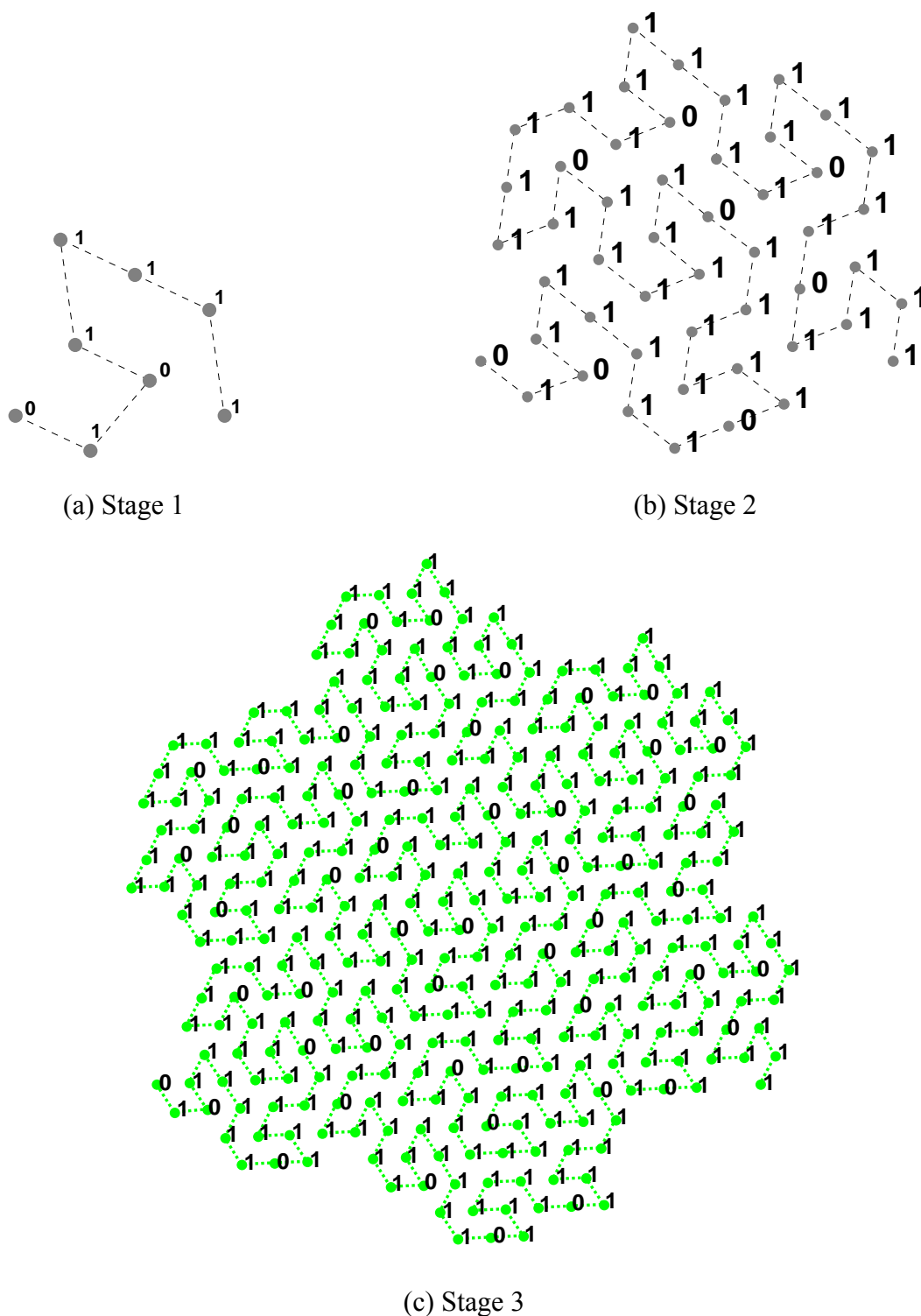


Figure 36 Element location for the (a) stage 1, (b) stage 2, and (c) stage 3 Peano-Gosper fractal arrays. A uniform spacing of d_{\min} is assumed between consecutive arrays elements which is the same for each stage, minimum spacing is $\lambda/2$, maximum current excitation is one.

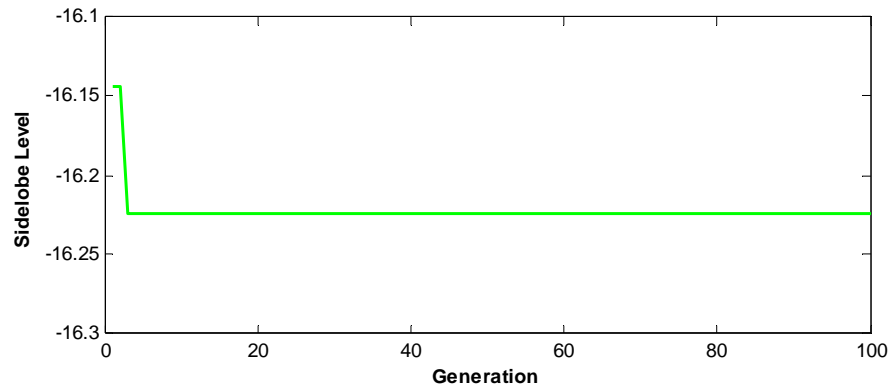


Figure 37 Evolution diagram of Genetically Optimized a Stage3: Peano-Gosper Fractal Array, minimum spacing is $\lambda/2$, maximum current excitation is one.

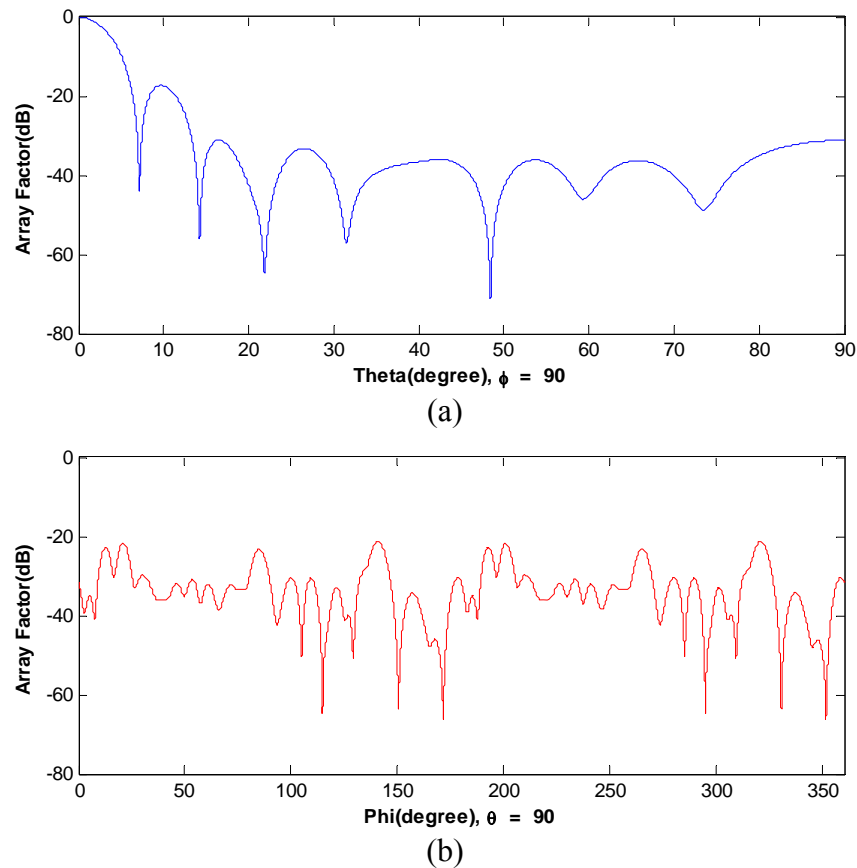
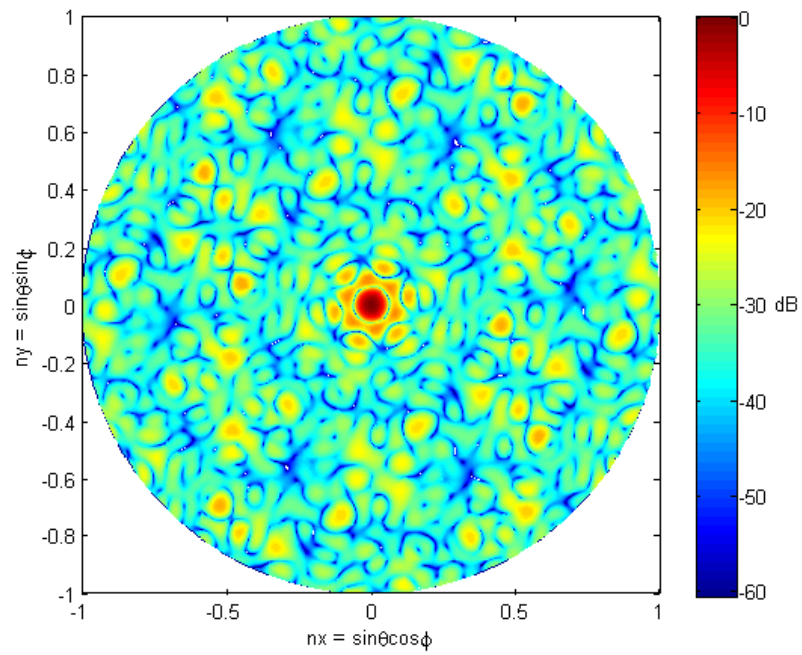
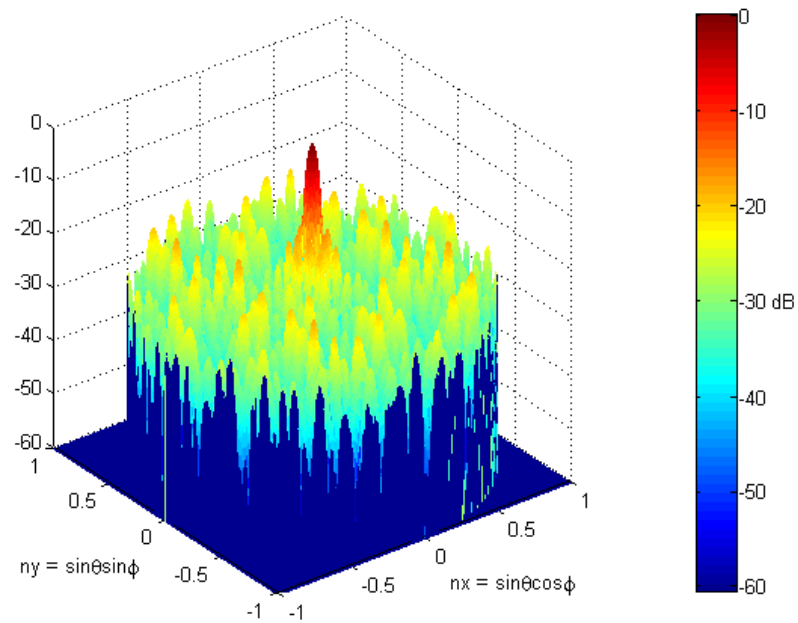


Figure 38. Plot of the normalized stage 3 Peano-Gosper fractal array, genetically optimized array factor versus (a) ϕ for $\theta = 90^\circ$ and (b) θ for $\phi = 90^\circ$ where minimum distance equal $\lambda/2$ and maximum current excitation equal one.



(a)



(b)

Figure 39 The normalized radiation pattern in dB for stage 3 of Peano-Gosper fractal array from Figure 36c with a minimum spacing is $\lambda/2$, maximum current excitation is one and main beam steered to $\theta = 0$ degrees and $\phi = 90^\circ$ degrees. (a) Radiation Pattern, and (b) Top View.

b. Minimum distance equal $\lambda/2$ and Maximum of current excitation equal ten

Consider the genetically optimized stage 1 Peano-Gosper fractal array and create higher order stage arrays (stage 3) with minimum spacing of $\lambda/2$ and maximum current excitation of 10. Figure 40 exhibits the Peano-Gosper fractal array for the stages of growth 1, 2 and 3, respectively. Figure 41 exhibits the sidelobe level of the Peano-Gosper fractal arrays for the stage of growth 3 versus generation. In addition, Figure 42 shows the plot of the normalized stage 3 Peano-Gosper fractal array, genetically optimized array factor versus (a) ϕ for (a) $\theta = 90^\circ$ and (b) θ for $\phi = 90^\circ$ where minimum distance equals $\lambda/2$ and maximum current excitation equals ten.

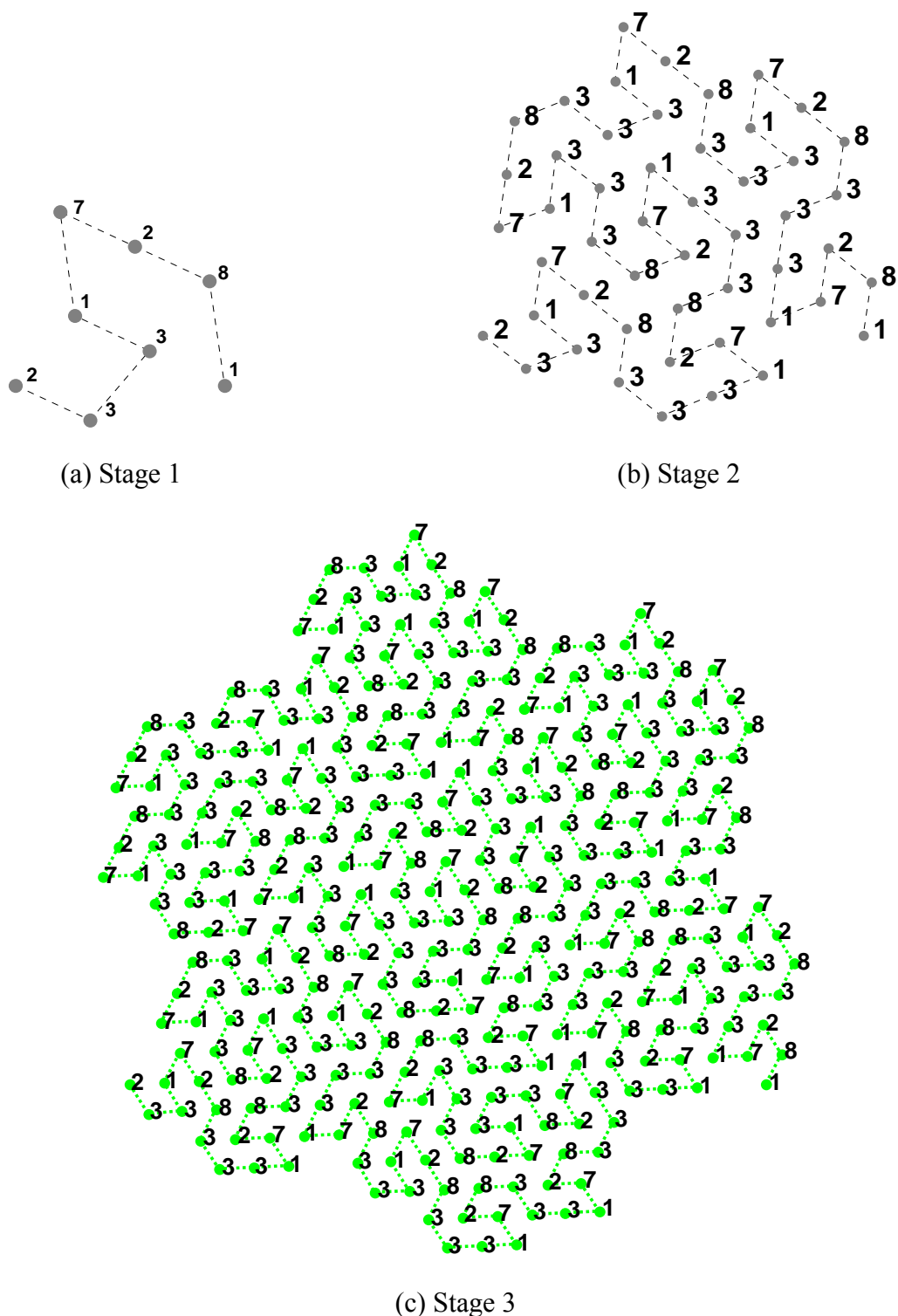


Figure 40. Element location for the (a) stage 1, (b) stage 2, and (c) stage 3 Peano-Gosper fractal arrays. A uniform spacing of d_{\min} is assumed between consecutive arrays elements which is the same for each stage, minimum spacing is $\lambda/2$, maximum current excitation is ten.

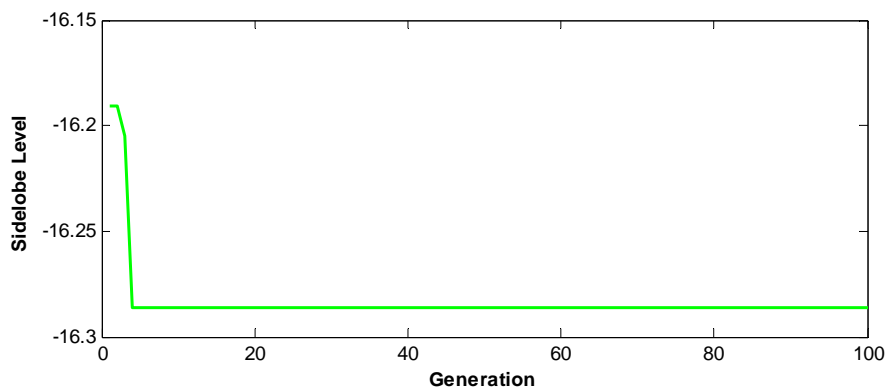


Figure 41 Evolution diagram of Genetically Optimized a Stage3: Peano-Gosper Fractal Array, minimum spacing is $\lambda/2$, maximum current excitation is ten.

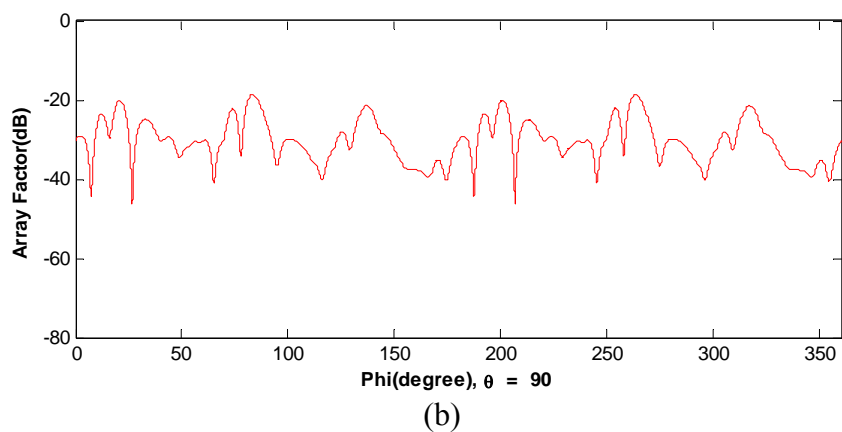
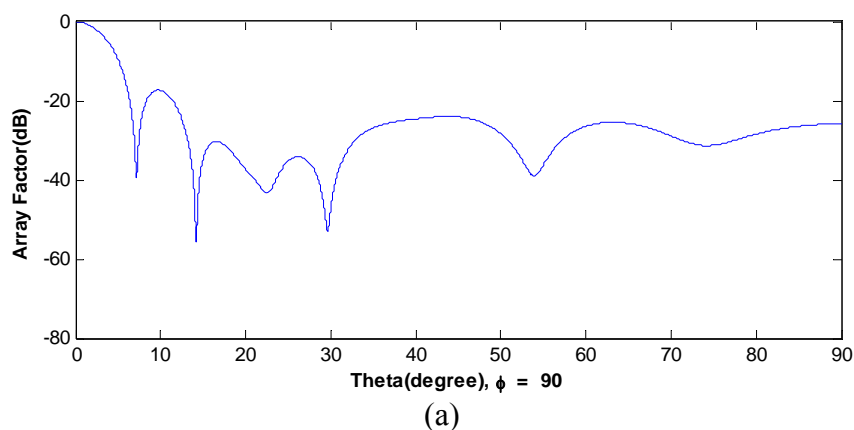
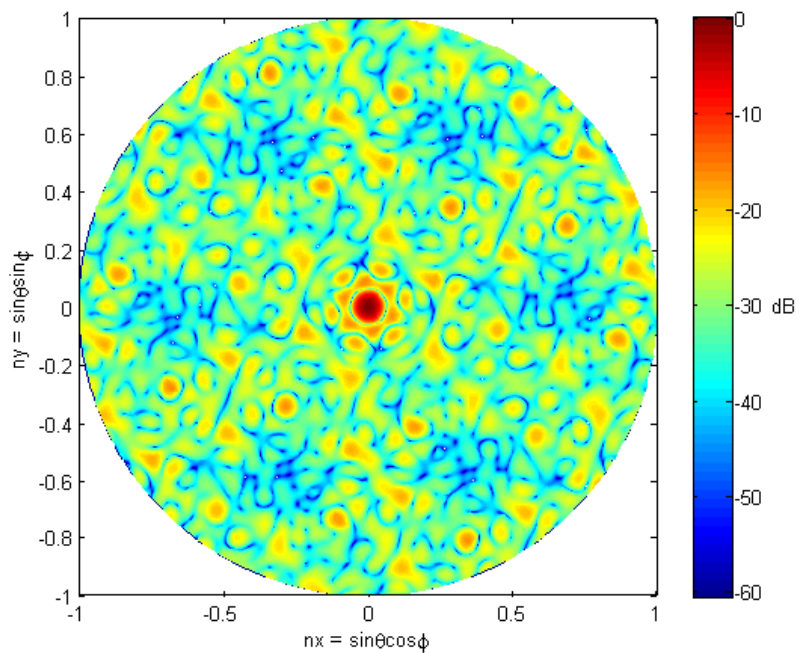
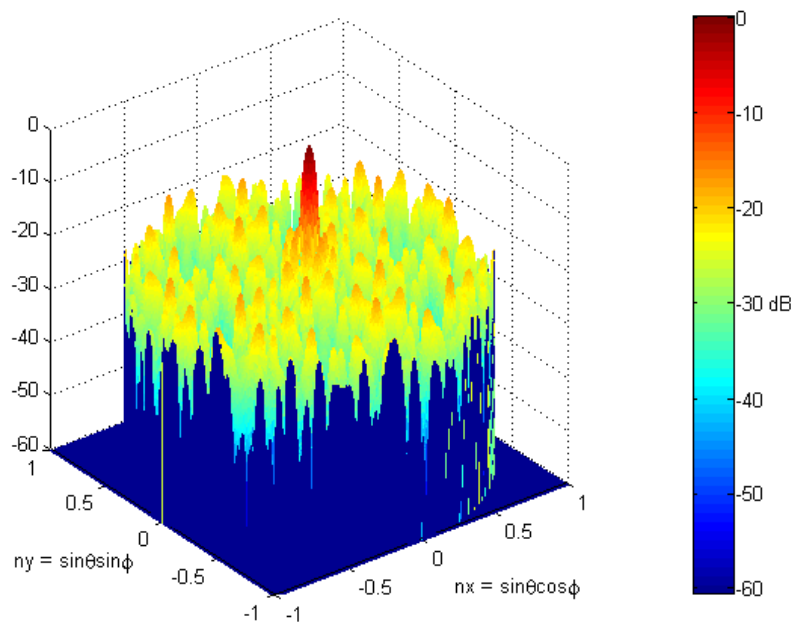


Figure 42 Plot of the normalized stage 3 Peano-Gosper fractal array, genetically optimized array factor versus (a) ϕ for $\theta = 90^\circ$ and (b) θ for $\phi = 90^\circ$ where minimum distance equal $\lambda/2$ and maximum current excitation equal ten.



(a)



(b)

Figure 43 The normalized radiation pattern in dB for stage 3 of Peano-Gosper fractal array from Figure 40c with a minimum spacing is $\lambda/2$, maximum current excitation is ten and main beam steered to $\theta = 0$ degrees and $\phi = 90^\circ$ degrees. (a) Radiation Pattern, and (b) Top View.

c. Minimum distance equal λ and Maximum of current excitation equal one

Consider the genetically optimized stage 1 Peano-Gosper fractal array and create higher order stage arrays (stage 3) with minimum spacing of λ and maximum current excitation of 1. Figure 44 exhibits the Peano-Gosper fractal array for the stages of growth 1, 2 and 3, respectively. Figure 45 exhibits the sidelobe level of the Peano-Gosper fractal arrays for the stage of growth 3 versus generation. In addition, Figure 46 shows the plot of the normalized stage 3 Peano-Gosper fractal array, genetically optimized array factor versus (a) ϕ for (a) $\theta = 90^\circ$ and (b) θ for $\phi = 90^\circ$ where minimum distance equals λ and maximum current excitation equals one.

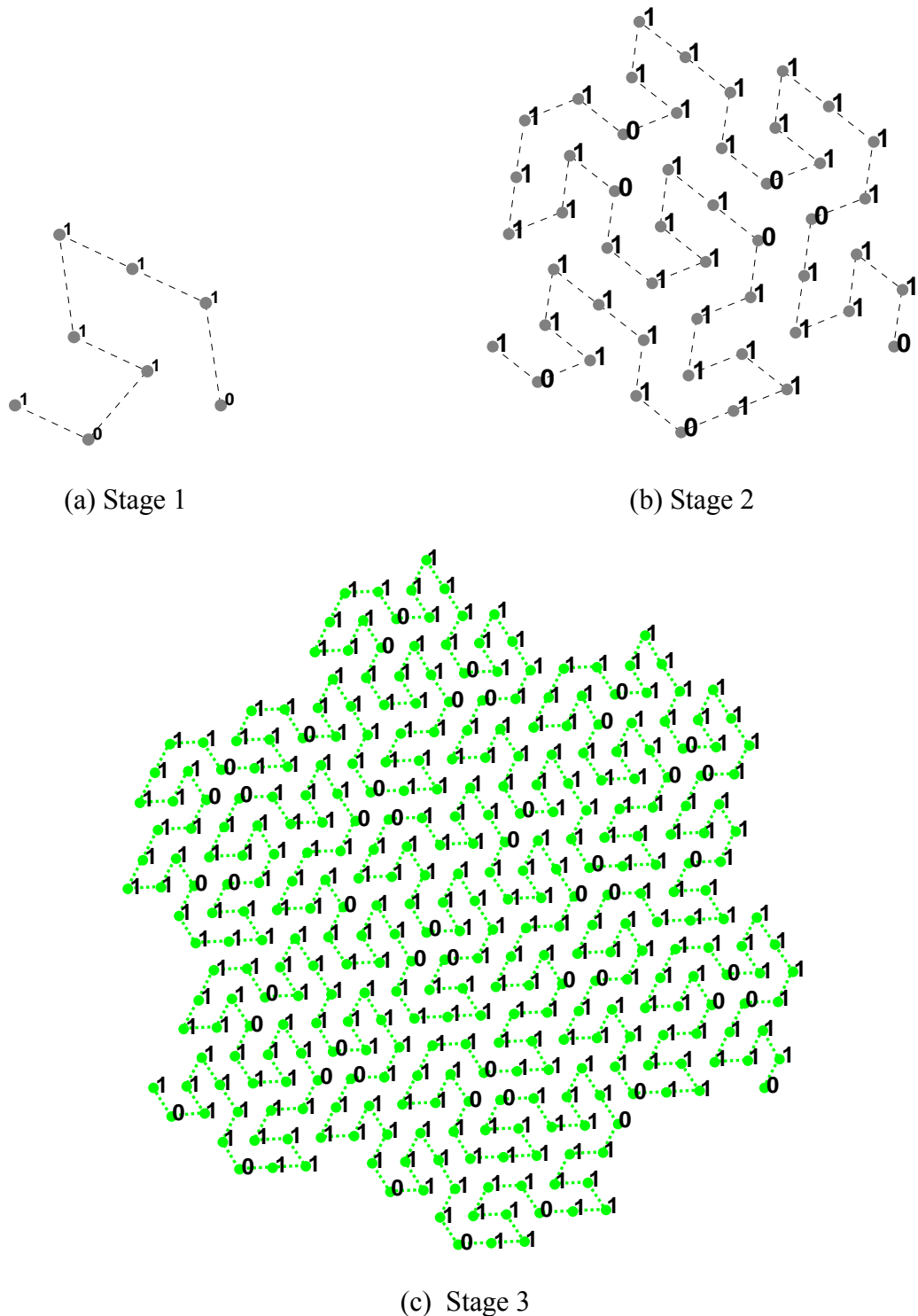


Figure 44 Element location for the (a) stage 1, (b) stage 2, and (c) stage 3 Peano-Gosper fractal arrays. A uniform spacing of d_{\min} is assumed between consecutive arrays elements which is the same for each stage, minimum spacing is λ , maximum current excitation is one.

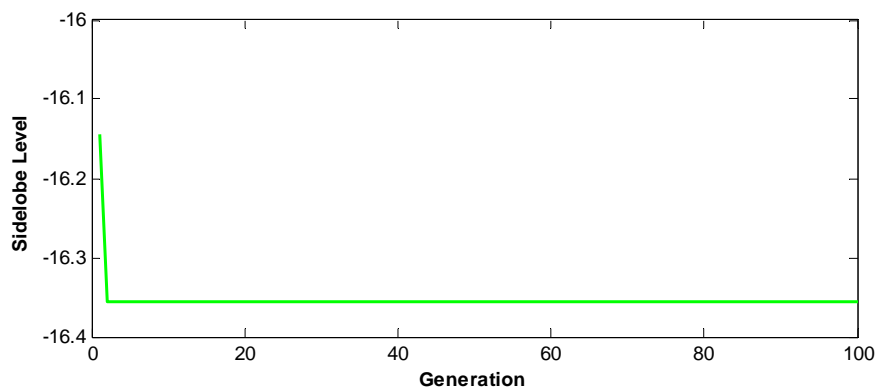


Figure 45 Evolution diagram of Genetically Optimized a Stage3: Peano-Gosper Fractal Array, minimum spacing is λ , maximum current excitation is one.

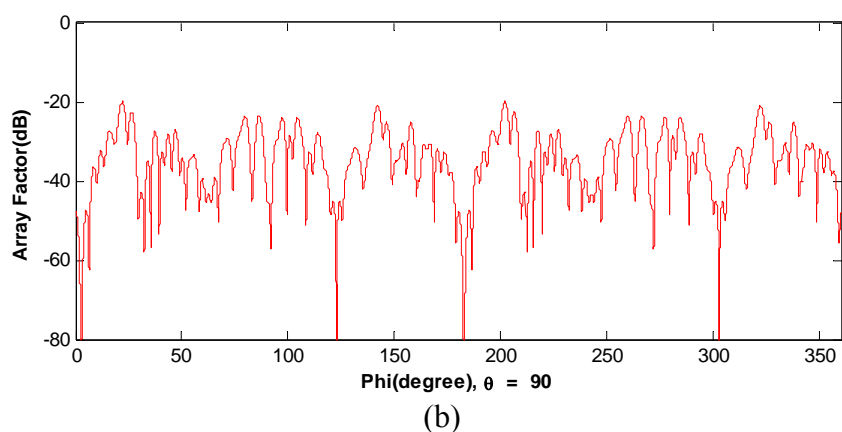
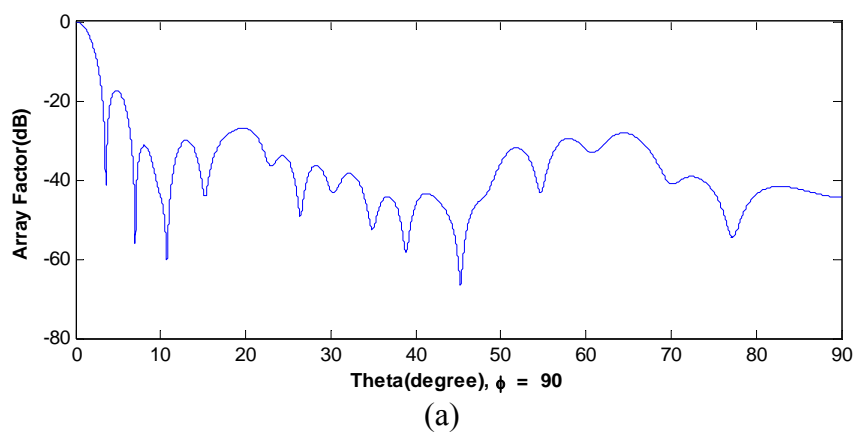
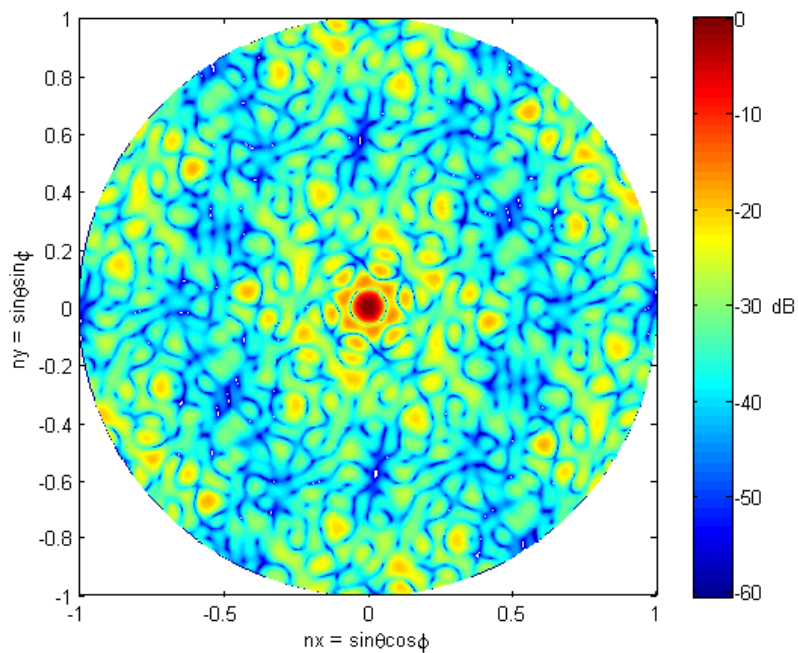
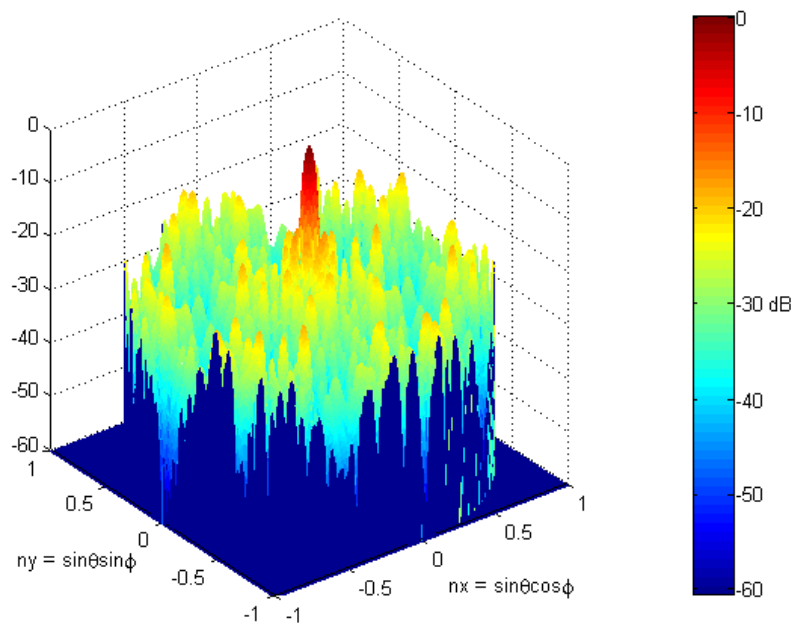


Figure 46 Plot of the normalized stage 3 Peano-Gosper fractal array, genetically optimized array factor versus (a) ϕ for $\theta = 90^\circ$ and (b) θ for $\phi = 90^\circ$ where minimum distance equal λ and maximum current excitation equal one.



(a)



(b)

Figure 47 The normalized radiation pattern in dB for stage 3 of Peano-Gosper fractal array from Figure 44c with a minimum spacing is λ , maximum current excitation is one and main beam steered to $\theta = 0$ degrees and $\phi = 90^\circ$ degrees. (a) Radiation Pattern, and (b) Top View.

d. Minimum distance equal λ and Maximum of current excitation equal ten

Consider the genetically optimized stage 1 Peano-Gosper fractal array and create higher order stage arrays (stage 3) with minimum spacing of $\lambda/2$ and maximum current excitation of 10. Figure 48 exhibits the Peano-Gosper fractal array for the stages of growth 1, 2 and 3, respectively. Figure 49 exhibits the sidelobe level of the Peano-Gosper fractal arrays for the stage of growth 3 versus generation. In addition, Figure 50 shows the plot of the normalized stage 3 Peano-Gosper fractal array, genetically optimized array factor versus (a) ϕ for (a) $\theta = 90^\circ$ and (b) θ for $\phi = 90^\circ$ where minimum distance equals $\lambda/2$ and maximum current excitation equals ten.

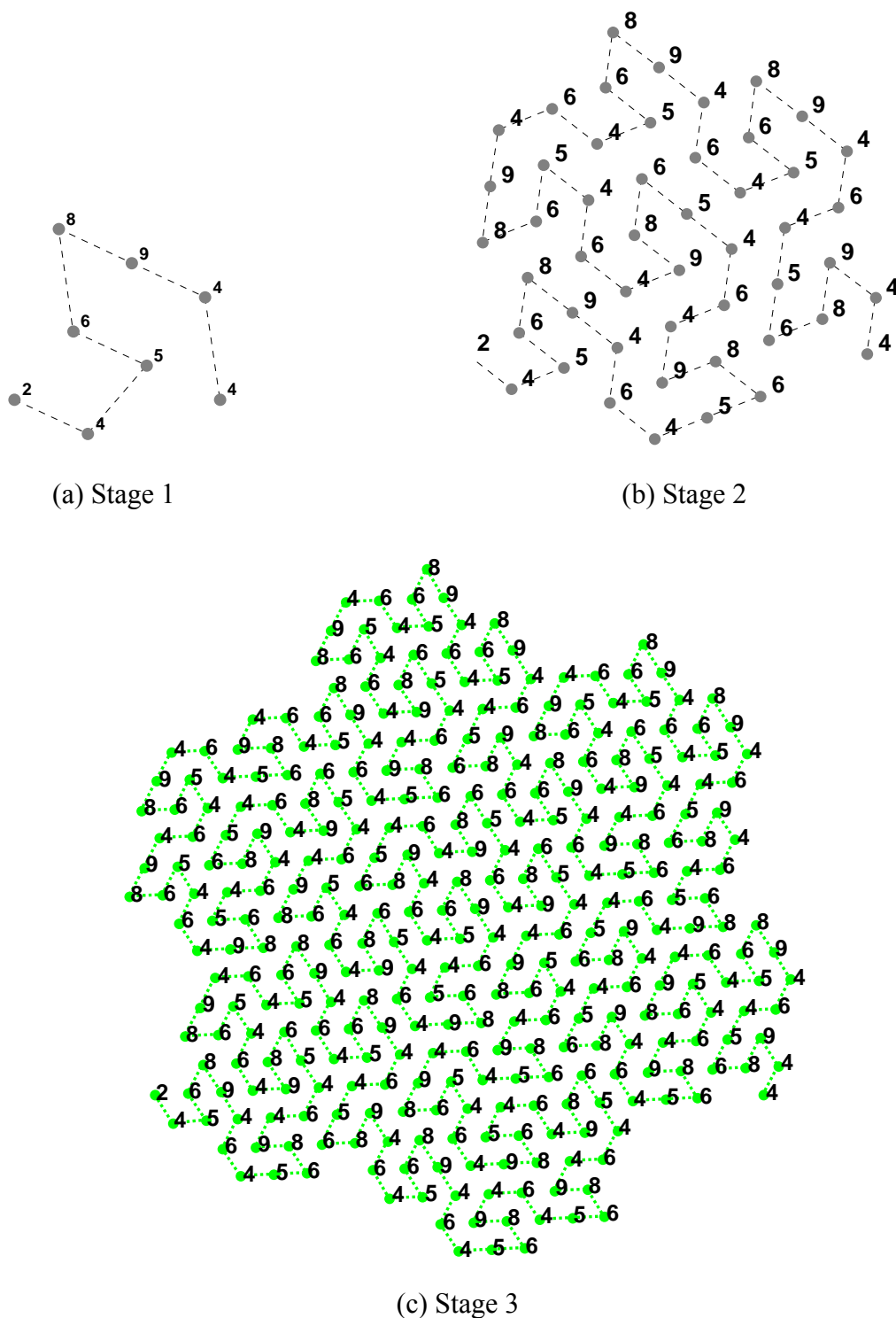


Figure 48 Element location for the (a) stage 1, (b) stage 2, and (c) stage 3 Peano-Gosper fractal arrays. A uniform spacing of d_{\min} is assumed between consecutive arrays elements which is the same for each stage, minimum spacing is λ , maximum current excitation is ten.

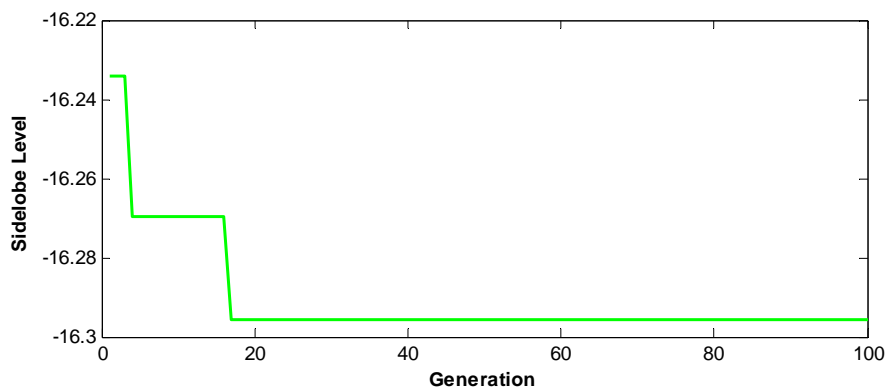


Figure 49 Evolution diagram of Genetically Optimized a Stage3: Peano-Gosper Fractal Array, minimum spacing is λ , maximum current excitation is ten.

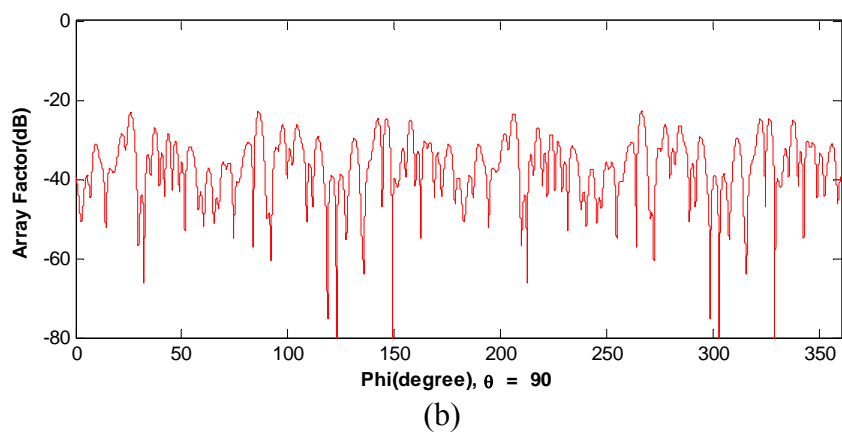
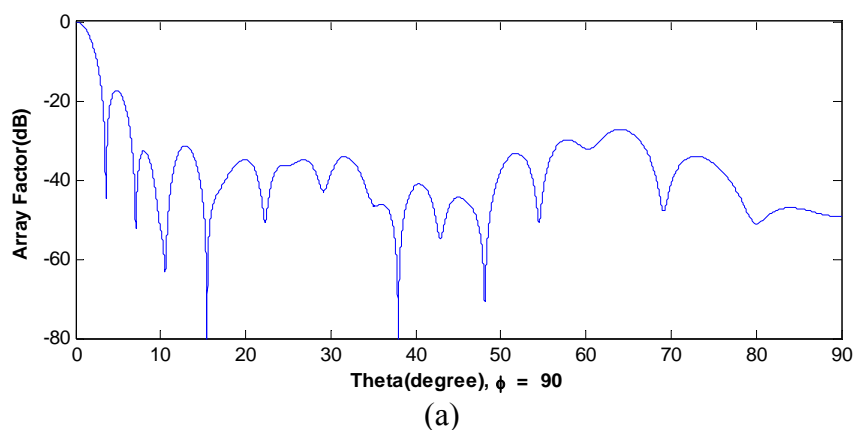
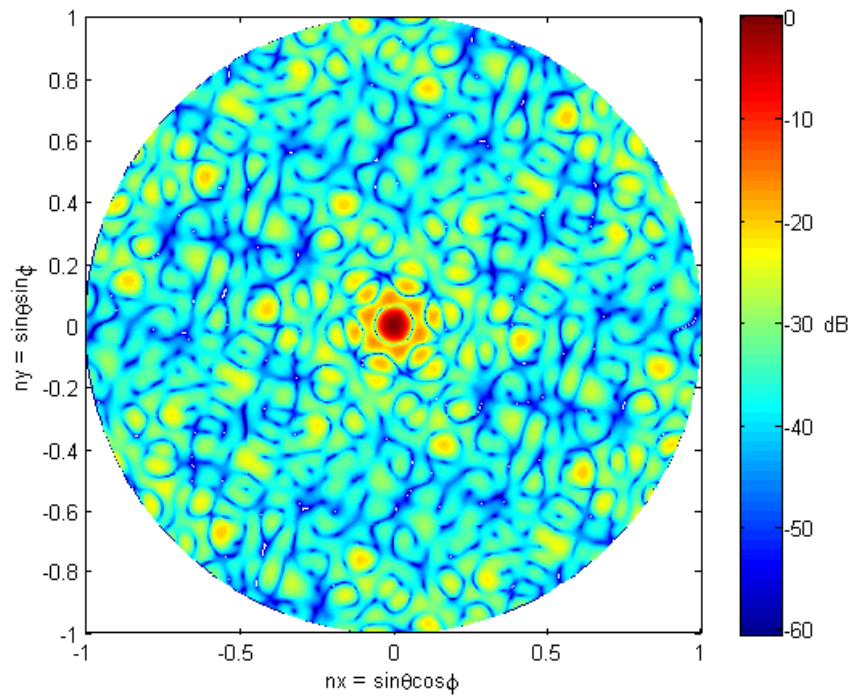
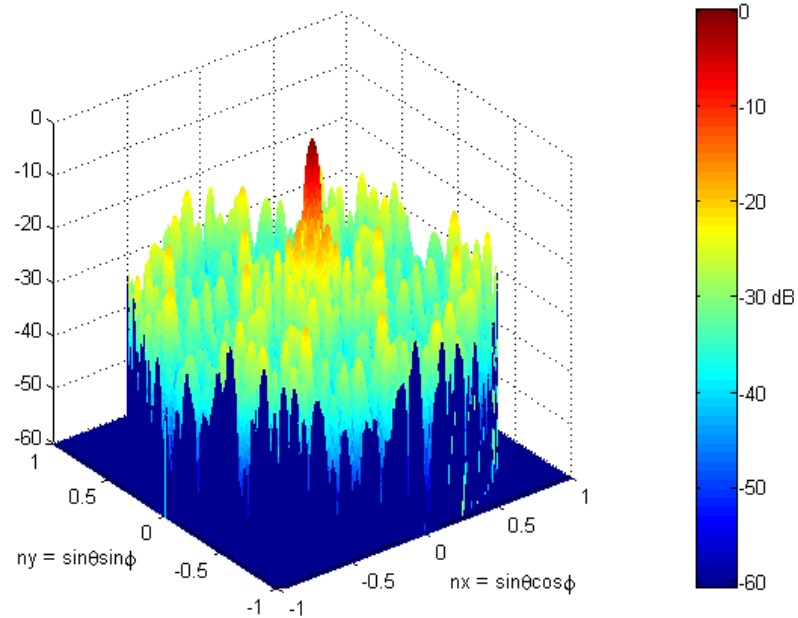


Figure 50 Plot of the normalized stage 3 Peano-Gosper fractal array, genetically optimized array factor versus (a) ϕ for $\theta = 90^\circ$ and (b) θ for $\phi = 90^\circ$ where minimum distance equal λ and maximum current excitation equal ten.



(a)



(b)

Figure 51 Top view of the normalized radiation pattern in dB for stage of Peano-Gosper fractal array of isotropic elements from Figure 48c with a minimum spacing is λ , maximum current excitation is ten and main beam steered to $\theta = 0$ degrees and for $\phi = 90^\circ$ degrees.

Regarding to Figures 19 to 51, comparison of the sidelobe levels in dB of the genetically optimized stage 3 Peano-Gosper fractal array with different parameters for both approaches is summarized in Table 1.

Table 1 Comparison of the sidelobe levels in dB of the genetically optimized stage 3 Peano-Gosper fractal arrays with different parameters for both approaches.

Approach	Minimum distance	Maximum current excitation	Sidelobe Level
1	0.5	1	-18.05
1	0.5	10	-18.04
1	1	1	-17.10
1	1	10	-19.04
3	0.5	1	-16.22
3	0.5	10	-16.29
3	1	1	-16.35
3	1	10	-16.29

CONCLUSION AND RECOMMENDATION

In this thesis, the optimization of antenna arrays is presented. For both approaches, antenna elements are strategically arranged uniformly on the Peano-Gosper fractal array. However, the relative current excitation also affects the performance of the Peano-Gosper fractal array. Then, we run genetic algorithm for optimizing the Peano-Gosper fractal array for 100 generations (iterations). It is empirically found that genetic algorithm can reduce the sidelobe levels to acceptable levels.

Although genetic algorithm performs well in optimization, its drawback is, like other optimization techniques, that its optimization process is time-consuming. Hence, our future work will focus on improving the speed of genetic algorithm to optimize antenna array synthesis.

LITERATURE CITED

- Balanis, C 2005. **Antenna Theory: Analysis and Design**. John Wiley and Sons, Inc. New York.
- Bogard, J. N., D. H. Werner, and P. L. Werner 2004. A Comparison of the Peano-Gosper Fractile Array with the Regular Hexagonal Array. **Microwave and Optical Technology Letters**, Vol. 43, No. 6: 524-526.
- Bondarenko, N. and Y.V. Mikhailova, 2005. Radiation Pattern Synthesis for Arrays Based on Soerpinski Gasket. **KORUS'2005**.
- Bray, M., G., D. H. Werner, D. W. Boeringer and D. W. Machuga 2002. Optimization of Thinned Aperiodic Linear Phased Arrays Using Genetic Algorithms to Reduce Grating Lobes During Scanning. **IEEE Transactions on Antennas and Propagation**, Vol. 50, No.11: 2919-2924.
- Falconer, K. 2003. **Fractal Geometry Mathematical Foundations and Applications** 2nd Edition, Wiley.
- Hansen, R.C. 2003. **Phased Array Antennas**. John Wiley and Sons, Inc. New York.
- Haupt, R. L. 2003. Thinned Arrays Using Genetic Algorithms. **IEEE Transactions on Antennas and Propagation**, Vol. 42, No.8 : 2008-2018.
- Haupt, R. L. 1995. An Introduction to Genetic Algorithms for Electromagnetics **IEEE Antennas and Propagation Magazine**, Vol. 37, No.2: 7-15
- Haupt, R. L. and S. E. Haupt. 2003. **Practical Genetic Algorithms**. John Wiley and Sons, Inc. New York.
- Johnson, M. and Y. Rahmut-Samii 1997. Genetic Algorithms in Engineering Electromagnetics. **IEEE Antennas and Propagation Magazine**, Vol. 39, No.4: 7-15, Aug.

- Kim, Y. and D. L. Jaggard 1986. The Fractal Random Array. **Proceeding of the IEEE**, Vol. 74, 9: 1278-1280
- Kraus, J., D. Ronald and J. Marhefka, 2003. **Antennas for All Applications**. McGraw-Hill
- Kuhirun, W. 2003. **A New Design Methodology for Modular Broadband Arrays based on Fractal Tailings**. Ph.D. Thesis, the Pennsylvania State University at University Park USA.
- Kuhirun, W., T..Jariyanorawiss, M. Polpasee, and N. Homsup 2004. Solving for Current Distribution Using Gauss-Seidel Iteration and Multigrid Method. **Proceedings of the International Conference in ECTI**, Thailand.
- Mandelbrot, B.B. 1983. **The Fractal Geometry of Nature**. John Wiley and Sons, Inc. New York.
- Massa, A., M. Donelli, Francesco G.B. De Nataale, Salvatore Caorsi and Andrea Lommi 2004. Planar Antenna Array Control With Genetic Algorithms and Adaptive Array Theory. **IEEE Transactions on Antennas and Propagation**, Vol. 52, No.11: 2919-2924.
- Petko, J. S. and D. H. Wener 2005. The Evolution of Optimal Linear Polyfractal Arrays Using Genetic Algorithms. **IEEE Transactions on Antennas and Propagation**, Vol. 53, No.11: 3604-3615.
- Polpasee, M. and N. Homsup 2006. Optimize Directivity Pattern for Arrays by Using Genetic Algorithms Based on Planar Fractal Arrays. **Proceedings of the International Conference in ISCIT**, Thailand.
- Polpasee, M. and N. Homsup 2006. Optimized low sidelobe level of Peano-Gosper Fractal Arrays Synthesis Using Genetic Algorithms. **Proceedings of the International Conference in ECTI**, Thailand.

- Polpasee, M. and N. Homsup 2006. Peano-Gosper Fractal Array Synthesis Using Genetic Algorithms. **Ocean 2006 IEEE Asia Pacific**, Singapore
- Polpasee, M., W. Kuhirun and N. Homsup 2005. Analysis of Fractal Arrays Generated using a 3x3 Subarray Generator. **Proceedings of the International Conference in ISCIT**, China.
- Polpasee, M., N. Homsu and W. Kuhirun 2005. Analysis of Fractal Arrays Generated using a 3x3 Subarray Generator. **Proceedings of the International Conference in ECTI**, Thailand.
- Soltankarimi, F., J. Nourinia and Ch.Ghobadi 2004. Sidelobe Level Optimization in Phased Array Antennas Using Genetic Algorithm. **ISSSTA 2004**.
- Villegas, F. J., T. Cwik, Y. Rahmat-Samii and Majid Manteghi 2004. A Parallel Electromagnetic Genetic-Algorithm Optimization(EGO) Application for Patch Antenna Design. **IEEE Transactions on Antennas and Propagation**, Vol. 52, No.9: 2424-2435.
- Vinoy, K.J. 2002. **Fractal Shaped Antenna Elements for Wide-and-Multi Band Wireless Application**. Ph.D. Thesis, The Pennsylvania State University at University Park USA.
- Virunha, P., M. Polpasee and N. Homsup 2006. Optimized Directivity of Square-Planar Fractal Arrays Using Genetic Algorithms. **Ocean 2006 IEEE Asia Pacific**, Singapore.
- Wener, D. H., K.C. Anusko and P.L. Werner 1999 The Generation of Sum and Difference Patterns Using Fractal SubArrays **Microwave And Optical Technology Letters**, Vol. 22, No. 1: 524-526.
- Wener, D. H., and R. Mittra 2000. **Frontiers in Electromagnetics**. IEEE Press.

- Wener, D. H., R. L. Haupt and P. L. Werner 1999. Fractal Antenna Engineering: The Theory and Design of Fractal Antenna Arrays. **IEEE Antennas and Propagation Magazine**, Vol. 41, No.5: 37-59.
- Wener, D. H and P. L. Werner, 1999. A General Class of Self-Scalable and Self-Similar Arrays.
- Wener, D. H., W. Kuhirun, and P. L. Werner 2004. Fractile Arrays: A New Class of Tiled Arrays With Fractal Boundaries. **IEEE Transactions on Antennas and Propagation**, Vol. 52, No.8: 2008-2018.
- Wener, D. H., W. Kuhirun, and P. L. Werner 2005. The Peano-Gosper Fractal Array. **IEEE Transactions on Antennas and Propagation**, Vol. 51, No.8: 2063-2072.
- Yan, K. and Y. Lu, 1997. Sidelobe Reduction in Array-Pattern Synthesis Using Genetic Algorithm. **IEEE Transactions on Antennas and Propagation**, Vol. 45, No.7: 1117-1122.
- Zhu, J., A. Hoorfar and N. Engheta 2004. Peano Antennas. **IEEE Antennas and Wireless Propagation Letters**. Vol.3.

CURRICULUM VITAE

NAME	Mr. Meta Polpasee
BIRTH DATE	December 1, 1980
BIRTH PLACE	Bangkok, Thailand
EDUCATION	YEAR INSTITUTION DEGREE/DIPLOMA
	2002 Kasetsart University B.Eng. (Electrical)

PUBLICATION

Polpasee, M. ,N.Homsup And P. Virunha “Optimize Directivity Pattern for Arrays by Using Genetic Algorithms Based on Planar Fractal Arrays” in Proceedings of the International Conference in ISCIT, Bangkok, May 2007

Polpasee, M. and N.Homsup “Peano-Gosper Fractal Array Synthesis Using Genetic ALgorithms” Ocean 2006 IEEE Asia Pacific, Singapore, May 2006

Virunha, P., M.Polpasee and N.Homsup “Optimized Directivity of Square-Planar Fractal Arrays Using Genetic Algorithms” Ocean 2006 IEEE Asia Pacific, Singapore, May 2006

Polpasee, M. and N.Homsup “Optimized low sidelobe level of Peano-Gosper Fractal Arrays Synthesis Using Genetic Algorithms” in Proceedings of the International Conference in ECTI, Ubonratchathani, May 2006

Polpasee, M, W. Kuhirun and N.Homsup "Analysis of Fractal Arrays Generated using a 3x3 Subarray Generator", in Proceedings of the International Conference in ISCIT, China , Oct 2005.

Polpasee, M, N.Homsup and W.Kuhirun "Analysis Fractal Array based on 3x3 Sub Array Generator, Pattaya, in Proceedings of the International Conference in ECTI, Pattaya, May 2005.

Kuhirun, W., T.Jariyanorawiss, M.Polpasee, and N.Homsup, "Solving for Current Distribution Using Gauss-Seidel Iteration and Multigrid Method" in Proceedings of the International Conference in ECTI, Pattaya, May 2004.